Observed and modeled surface Lagrangian transport between coastal regions in the Adriatic Sea with implications for marine protected areas

Daniel F. Carlson[a,*], Annalisa Griffa[b], Enrico Zambianchi[c], Giuseppe Suaria[b], Lorenzo Corgnati[b], Marcello G. Magaldi[b,d], Pierre-Marie Poulain[e], Aniello Russo[f,g], Lucio Bellomo[h], Carlo Mantovani[b], Paolo Celentano[c], Anne Molcard[h], Mireno Borghini[b]

[a]*Department of Earth, Ocean, and Atmospheric Sciences, The Florida State University, Tallahassee FL, USA*
[b]*CNR-ISMAR, La Spezia, Italy*
[c]*DiST, Università degli Studi di Napoli "Parthenope" and CoNISMa, Napoli, Italy*
[d]*Department of Earth and Planetary Sciences, Johns Hopkins University, Baltimore MD, USA*
[e]*Istituto Nazionale di Oceanografia e di Geofisica Sperimentale (OGS), Trieste, Italy*
[f]*DiSVA, Università Politecnica delle Marche, Ancona, Italy*
[g]*Present Address: NATO-STO Centre for Maritime Research and Experimentation, La Spezia, Italy*
[h]*University of Toulon, UMR7294, CNRS/INSU, IRD - Mediterranean Institute of Oceanography (MIO), UM 110, 83957 La Garde, France*

Abstract

Surface drifters and virtual particles are used to investigate transport between seven coastal regions in the central and southern Adriatic Sea to estimate the degree to which these regions function as a network. Alongshore coastal currents and cyclonic gyres are the primary circulation features that connected regions in the Adriatic Sea. The historical drifter observations span 25 years and, thus, provide estimates of transport between regions

*Dept. of Earth, Ocean, and Atmospheric Science, FSU, Tallahassee FL
Email address: danfcarlson@gmail.com (Daniel F. Carlson)
1*

realized by the mean surface circulation. The virtual particle trajectories and a dedicated drifter experiment show that southeasterly Sirocco winds can drive eastward cross-Adriatic transport from the Italian coast near the Gargano Promontory to the Dalmatian Islands in Croatia. Southeasterly winds disrupt alongshore transport on the west coast. Northwesterly Mistral winds enhanced east-to-west transport and resulted in stronger southeastward coastal currents in the western Adriatic current (WAC) and export to the northern Ionian Sea. The central Italian regions showed strong connections from north to south, likely realized by alongshore transport in the WAC. Alongshore, downstream transport was weaker on the east coast, likely due to the more complex topography introduced by the Dalmatian Islands of Croatia. Cross-Adriatic connection percentages were higher for east-to-west transport. Cross-Adriatic transport, in general, occurred via the cyclonic sub-gyres, with westward (eastward) transport observed in the northern (southern) arms of the central and southern gyres.
Keywords: Surface Lagrangian Transport, Adriatic Sea, Surface Drifters, ROMS, Particle Tracking, Marine Protected Areas

1. Introduction

The European Union (EU) mandated the formation of networks of marine protected areas (MPAs) to achieve good environmental status in EU waters by 2020 (Fenberg et al., 2012). Ocean currents play a fundamental role in the dispersal stage of many marine organisms (Cowen et al., 2007; Gawarkiewicz et al., 2007; Pineda et al., 2007; Treml et al., 2008), and transport by ocean currents can affect the degree to which MPAs function as a network (Corell

et al., 2012; Largier, 2003; Puckett et al., 2014). However, the small sizes of marine larvae and propagules complicate direct tracking from spawning to settlement/recruitment (Gaines et al., 2007; Largier, 2003), though progress has been made in this area (Langård et al., 2015). Drifters and/or virtual particle trajectories often serve as simplified indicators of larval and propagule pathways in studies of hydrodynamic connectivity (Lugo-Fernández et al., 2001; Tang et al., 2006; Tilburg et al., 2006; Hare et al., 2002; Andrello et al., 2013; Rossi et al., 2014; Di Franco et al., 2012a; Pujolar et al., 2013).

This paper, therefore, uses surface drifters and virtual particles to investigates surface transport between regions in the central and southern Adriatic Sea (Fig. 1a) to determine if Lagrangian transport could impact the degree to which these MPAs and their surroundings function as a coherent network. This paper focuses entirely on surface Lagrangian transport of passive drifters and virtual particles and, therefore, is most applicable to the study of buoyant, passive tracers. While we make no attempt to apply our results to the dispersal of a specific species, this study will provide valuable information for resource managers and decision makers about average transit times and the potential for exchange between MPAs and their surroundings in the Adriatic Sea on ecologically relevant timescales (see section 2.4).

First, we use CODE-type (Davis, 1985) surface drifters deployed in the Adriatic Sea from 1990 to 2015 to compute transit times and the connection percentage between regions (see section 2.4). The drifters quantify the role of the surface circulation, summarized in section 1.1, in connecting regions in the Adriatic Sea. While the drifter data provide important quantitative metrics of transport between regions, relatively few data are available and

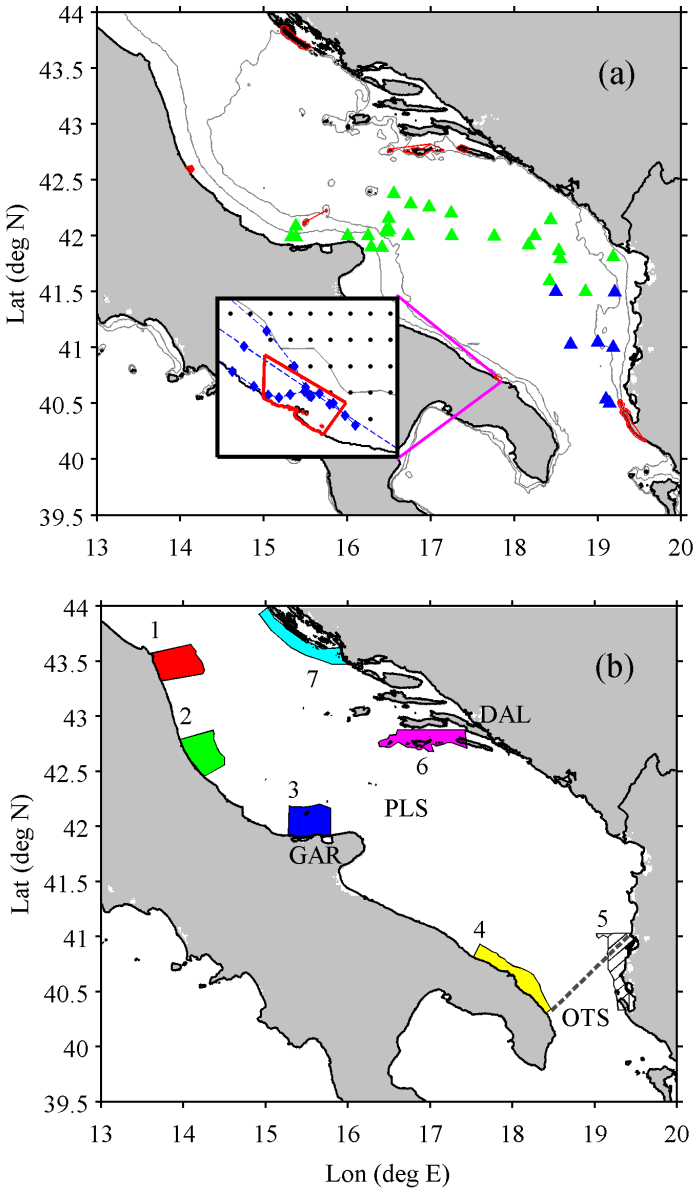

Figure 1: (a) The Adriatic Sea with the CoCoPro drifter launch locations in 2013 and 2015 denoted by green and blue triangles, respectively. MPA boundaries are plotted in red. The 50 m and 100 m isobaths are plotted in grey. Inset: The Torre Guaceto MPA boundary is plotted in red, along with the ROMS grid points in the vicinity (black) and the three drifter trajectories that passed through the MPA (blue). (b) Coastal regions used for transport assessments: 1) Conero (Italy); 2) Torre del Cerrano (Italy); 3) Isole Tremiti (Italy); 4) Torre Guaceto (Italy); 5) Karaburun (Albania); 6) Mljet (Croatia); 7) Kornati (Croatia). The Dalmatian Islands (DAL), Palagruza Sill (PLS), Gargano Promontory (GAR), and Otranto Strait (OTS) are also indicated. The dashed grey line denotes the southern boundary of the ROMS simulation.

the results are subject to well-documented biases due to drifter mortality (Falco et al., 2000; Poulain and Hariri, 2013) that are partially accounted for in our analysis methods (see section 2.4).

The second assessment uses a Regional Ocean Modelling System (ROMS; Shchepetkin and McWilliams (2005)) simulation of the Adriatic Sea during May–August 2013 and surface winds from the Consortium for Small-Scale Modelling (COSMO) atmospheric model (see section 2.7) to investigate the effects of wind forcing on transport between regions. We focus on the period May–August 2013 in order to validate virtual particle trajectories from the ROMS simulation with surface drifter trajectories from a dedicated deployment in the central Adriatic Sea (see section 2.2) during the same time. 115500 virtual particle trajectories (300 virtual particles released every 24 hr from 1 May to 17 July 2013 in five regions) enable computation of statistically robust connection percentages and mean transit times and provide useful qualitative information about transport pathways under different wind conditions. The virtual particle trajectories show that variable wind events do, in fact, influence surface Lagrangian pathways, and should be considered in resource management.

The remainder of this paper is organized as follows. Sections 1.1 – 1.2 review relevant studies of surface circulation and connectivity, respectively, in the Adriatic Sea. The regions, drifter data, ROMS and COSMO configurations, virtual particle tracking scheme, and analysis methods are described in section 2. Results are presented in section 3 and discussed in section 4. We summarize and conclude in section 5.

1.1. Review of surface transport in the Adriatic Sea

Cyclonic circulation dominates the large scales with northwestward flow on the east coast, in the east Adriatic current (EAC), and southeastward flow on the west coast, in the west Adriatic Current (WAC) (Poulain, 1999; Burrage et al., 2009) with significant variability observed over a range of scales, from climatic, seasonal, and synoptic scales (Maurizi et al., 2004). Smaller cyclonic gyres exist in the northern, central, and southern Adriatic (Poulain, 1999). At the synoptic to seasonal timescales considered in this study, the circulation varies in response to air-sea interaction, river runoff, and wind forcing. Wind forcing affects the surface mesoscale circulation and can influence the behavior of river plumes and coastal currents (Orlić et al., 1994; Burrage et al., 2009; Poulain, 1999).

Northwesterly Mistral winds prevail in summer, southeasterly Sirocco winds in winter, and cold, strong northeasterly Bora winds typically occur in winter (Pasarić et al., 2009; Orlić et al., 1994; Bignami et al., 2007). Summertime northwesterly winds tend to be weaker but more steady (Pasarić et al., 2009). Ursella et al. (2006) examined the response of drifters to wind forcing in the northern and central Adriatic Sea using over 120 drifters released from September 2002 – November 2003 and found that surface currents responded nearly instantaneously to the wind and were oriented within 15^o of the wind vector.

Po river discharge and transient wind forcing, drive the WAC (Bignami et al., 2007; Burrage et al., 2009; Magaldi et al., 2010). Northwesterly and southeasterly winds blow parallel to the coast and, if persistent, lead to downwelling or upwelling, respectively, on the Italian coast. The WAC responds to

downwelling-favorable winds by decreasing in width and increasing in vertical thickness (Magaldi et al., 2010; Burrage et al., 2009). Downwelling-favorable winds suppress the formation of instabilities in the WAC but relaxation of downwelling winds and transition to upwelling-favorable winds promote the formation of eddies and filaments through baroclinic instability as the WAC spreads offshore and decreases in vertical thickness (Magaldi et al., 2010; Poulain et al., 2004). Southeasterly winds can drive mixing (Pasarić et al., 2007; Magaldi et al., 2010) and have been observed to reverse the WAC (Orlić et al., 1994; Poulain et al., 2004).

Previous surface drifter studies in the Adriatic Sea examined the mesoscale surface circulation, its seasonal variability, and response to wind forcing (Poulain, 1999, 2001; Ursella et al., 2006; Falco et al., 2000). Poulain (1999) found that the influx of surface water from the Ionian Sea and cyclonic circulation around the SAP reached a minimum in spring while outflowing waters in the western Otranto Strait on the Italian coast reached their maximum. Falco et al. (2000) found increased transport between southern and northern regions during late summer and fall. Poulain (2001) observed that the WAC was slightly stronger in summer and faster in the south and well-defined gyres in summer and fall, with weaker mean currents in spring. Strong, short-lived wind forcing drives variability in the average surface transport (Pasarić et al., 2007; Magaldi et al., 2010; Poulain et al., 2004; Ursella et al., 2006).

1.2. Review of selected population connectivity studies

Relatively few connectivity studies in the Adriatic basin have been published, with most studies addressing local scale (10s to 100s of km) processes based on recruitment/settlement observations (Bussotti et al., 2011)

and otolith chemistry and genetics (Di Franco et al., 2012b). Lagrangian modelling studies of the entire Mediterranean Sea (e.g. Andrello et al., 2013; Rossi et al., 2014; Berline et al., 2014) used spatial resolutions of the same order as the Rossby radius of deformation in the Adriatic Sea (Paschini et al., 1993; Cushman-Roisin et al., 2007) and likely did not accurately resolve local dynamics. Higher resolution models have been used in the Adriatic Sea, but only to study a single MPA (Di Franco et al., 2012a; Pujolar et al., 2013).

Two studies of population connectivity of the white sea bream *Diplodus sargus sargus* in the Torre Guaceto (TG) MPA (Fig. 1a) and surroundings combined biological sampling with virtual Lagrangian particle tracking schemes (Di Franco et al., 2012a; Pujolar et al., 2013). Virtual particles were released in and around TG and tracked for 17 days (Di Franco et al., 2012a; Pujolar et al., 2013). Both studies found high genetic homogeneity and propagule supply over scales of 100 km north and south of TG. Their results showed limited retention within the TG MPA, with transport from north to south in the WAC and export to the northern Ionian Sea. The genetic homogeneity observed north of TG could be explained by transport of larvae from northern areas (Di Franco et al., 2012a; Pujolar et al., 2013). Alternatively, WAC reversal under strong, persistent southeasterly winds could result in transport from TG to the north (Di Franco et al., 2012a; Pujolar et al., 2013).

Andrello et al. (2013) found limited bidirectional connections in the Adriatic basin, with a low connection probability throughout the entire Mediterranean basin. Hydrodynamic provinces in the Mediterranean Sea computed

by Rossi et al. (2014) show that the Adriatic Sea contained two provinces, with the southern boundary of the northernmost province extending across the Palagruza Sill (see Fig. 1a). The southern province, on the other hand, encompassed the central and southern Adriatic Sea as well as the northern Ionian Sea. Berline et al. (2014) identified eco-regions in the Mediterranean Sea based solely on hydrodynamic connectivity. The eco-regions were consistent with the well-known surface circulation features, with the entire Adriatic Sea listed as one eco-region with a boundary at the Otranto Strait (Berline et al., 2014). The low connectivity found by Andrello et al. (2013) as well as the boundaries of the hydrodynamic provinces and eco-region in the Adriatic Sea could be explained by the inability of the $1/12^o$ models to adequately resolve variability in surface transport in the Adriatic Sea, where the first baroclinic deformation radius varies from 5–10 km (Paschini et al., 1993; Cushman-Roisin et al., 2007). Recently, Putman and He (2015) showed that model-based estimates of marine connectivity depend strongly on the temporal and spatial resolutions of the underlying velocity fields.

2. Data and methods

The present study, therefore, uses 25 years of surface drifter observations (see sections 2.1-2.2) and a high-resolution numerical model (2.5) to quantify transport between coastal regions. The drifter-based results provide an ensemble average of transport, presumably capturing transport under different conditions. Comparison of virtual trajectories and drifters shows that the high resolution model adequately reproduced surface conditions in the Adriatic during May–August 2013 (section 3.3).

2.1. Historical drifter data

360 CODE-type drifters that sampled the upper 1 m (Davis, 1985) were deployed in the Adriatic Sea and northern Ionian Sea from 1990 - 2015 (Poulain, 1999, 2001; Poulain and Hariri, 2013). We use only CODE drifters to ensure that differences in transport were not due to different water-following characteristics of the various drifter types in the historical drifter database. Historical drifter positions were interpolated using a kriging method, low-pass filtered, and subsampled at 6 hr intervals (see Poulain (1999, 2001); Poulain and Hariri (2013) for details).

2.2. CoCoPro surface drifter experiments

The CoCoPRO drifter experiments were conducted under the framework of the CoCoNET (Towards COast to COast NETworks of Marine Protected Areas Coupled with Sea-Based Wind Energy Potential) FP7 European project. The drifter experiments were designed to fulfill one of the goals of the CoCoNET project: to investigate the mechanisms driving physical dispersion and influencing surface transport pathways between MPAs in the Adriatic Sea, with an emphasis on cross-basin connections. In May 2013, twenty-six CODE drifters were deployed in the central Adriatic Sea from the Gargano Promontory, along the Palagruza Sill, into the southern Adriatic Pit, to the Croatian and Albanian coasts (Fig. 1). The CoCoPRO 2013 drifter data span the period May-July 2013. The CoCoPRO 2013 drifters reveal the influence of the WAC, the EAC, and the central and southern gyres, with export of drifters to the northern Ionian Sea on the western side of the Otranto Strait (Fig. 2). The CoCoPRO 2013 drifters are also used

to validate virtual particle trajectories computed using the ROMS velocities during the period May–July 2013. An additional seven CODE surface drifters were deployed 10-11 March 2015 in the southeastern Adriatic Sea (Fig. 1a). Drifter GPS positions were accurate to 10 m and were transmitted every 15 min. Raw data were edited to remove spikes and are available at http://www.coconet-fp7.eu.

2.3. Adriatic Sea regions

Actual MPA boundaries shown in Figure 1a enclose areas that are too small to conduct a transport study. Using the MPA boundaries and all 393 drifter trajectories (regardless of drifter lifetime), we find that 1-15 drifters passed through MPA boundaries. Only two of these drifters traveled between MPAs. Furthermore, the small sizes of the MPAs also prohibit the use of ROMS simulation due to the 5 m minimum depth used in the model. The Torre Guaceto MPA boundaries are shown in the inset in Figure 1a along with the three drifter trajectories that passed through the MPA boundaries to illustrate the restrictions imposed by the size and proximity to shore.

Therefore, to increase the number of drifter trajectories available for analysis and to enable the use of the model, we define seven equal-area (1270 km^2) regions to include one or more existing, or planned, MPAs in the central and southern Adriatic Sea and their surrounding areas, extending offshore to the 100 m isobath (Fig. 1b). We focus on the central and southern Adriatic as large-scale modelling studies have mixed results in this area, with some identifying it as a hydrodynamic province (Rossi et al., 2014) and an ecoregion (Berline et al., 2014) while others found limited connectivity in the basin (Andrello et al., 2013). Drifter results have shown that the central and

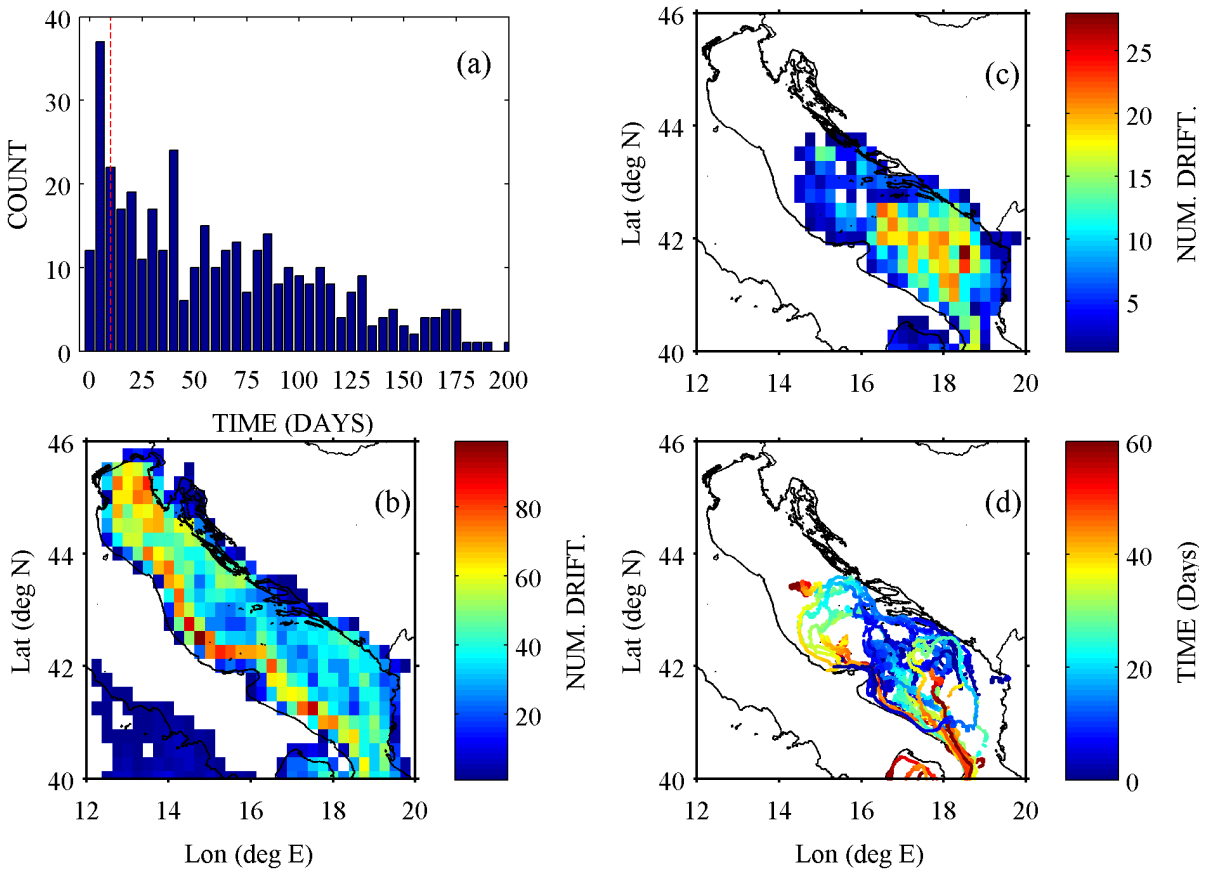

Figure 2: (a) Histogram of lifetimes of all drifter trajectories (historical and CoCoPRO) in the Adriatic Sea. The red vertical dashed line corresponds to 10 days. The densities of (b) historical CODE and (c) CoCoPRO 2013 and 2015 drifter measurements, computed as the number of non-consecutive entries and deployments in each 0.25^o bin. Note the different color scales for (b) and (c). (d) CoCoPRO 2013 drifter trajectories color coded to indicate time since deployment.

southern Adriatic can be characterized by two well-connected recirculation cells (gyres) (Poulain, 2001). This region was also specifically targeted by the CoCoNET project and the CoCoPRO drifter experiment. We make no effort to apply our results directly to spawning and recruitment/settlement of specific marine organisms. The results presented in this paper should be viewed as indications of offshore, mesoscale transport between coastal regions.

2.4. Drifter transport analysis methods

393 surface drifter trajectories, including the historical drifter database and the CoCoPRO drifters, were used to compute the connection percentage and transit time between each region pair, for a total of 42 source-destination combinations. The transit time is defined as the time from first exit from a source region to the time of first entry in a destination region. Transport between regions was quantified by computing the connection percentage, or the number of drifters that traveled to a destination region divided by the total number of drifters that left the source region. The 95% confidence interval around the connection percentage was computed using the Wilson Score (Agresti and Coull, 1998). The average transit time between regions was computed using a bootstrap estimate of the mean (Efron and Tibshirani, 1986) when at least 10 drifters connected the regions.

Drifter-derived metrics, in this case connection percentages and average transit times, must consider the bias introduced by the finite lifetime and non-uniform spatial distribution of the drifters (Falco et al., 2000; Poulain and Hariri, 2013). Historical drifter coverage was highest in the northern Adriatic and in the WAC (50-75 observations per $1/4\ ^{o}$ bin) with fewer observations in the central and southern parts of the basin (Fig. 2b). The CoCoPRO drifters

had fewer observations (33 total drifters) with maximal concentration in the southern Adriatic (Fig. 2c).

The bias introduced by finite drifter lifetimes was addressed by imposing minimum and maximum lifetime limits. Figure 2a shows that drifter lifetimes peaked at periods of 10 days or less. As a result, we required drifters to "live" *at least* 10 days after leaving a given source region. This requirement removed short-lived trajectories that could have exited a source region with very little lifetime remaining, thereby biasing the connection percentage towards lower values. Given that this paper is motivated by understanding surface transport at synoptic to monthly timescales relevant to the dispersal and recruitment of marine organisms, upper bounds on drifter lifetimes of 30 and 45 days were imposed, thereby removing biases introduced by short and long-lived drifters but also reducing the number of drifter trajectories available for analysis. In other words, the upper bounds removed connections, and their subsequent impacts on connection percentages and transit times that occurred over longer time scales (in some cases 80-100 days). Drifter lifetimes (Fig. 2a) suggest that transport estimates could be biased by the smaller set of long-lived trajectories, providing additional support for the lifetime limits of 30 days and 45 days.

Thus, the drifter analyses were performed considering three datasets: no maximum lifetime (L_0), 30-day lifetime limit (L_{30}), and 45-day lifetime limit (L_{45}). L_0 has no upper bound on drifter lifetimes, and therefore considers "asymptotic" ensemble averages. L_{30} and L_{45}, instead, set lifetime upper bounds at 30 and 45 days respectively, and, therefore, consider transport processes averaged over finite time scales. Timescales of 30 and 45 days cor-

respond to typical pelagic larval durations for several marine organisms in the Adriatic Sea and Mediterranean Sea (Shanks, 2009), and they are also relevant for studies of marine pollution. The 30 and 45 day timescales fall within the range employed in other studies of hydrodynamic connectivity in the Adriatic Sea (see section 1.2 and references therein). The L_0 timescale might be relevant for plastic litter transport, whose residence on the surface might be of the order of years, and for a wide variety of other asexual fragments, spores, propagules and dispersal stages with longer residence times in the water column.

2.5. AdriaROMS and virtual particle tracking

We use surface currents produced by AdriaROMS 4.0 (Russo et al., 2013a,b), the operational implementation of ROMS (Shchepetkin and McWilliams, 2005; Haidvogel et al., 2008) for the Adriatic Sea. The Hydro-Meteo-Clima Service of the Emilia Romagna Environmental Agency (SIMC-ARPA-ER, Bologna, Italy) manages AdriaROMS, as well as the numerical weather prediction system COSMO-I7, whose operational outputs allow the computation of air-sea fluxes (Russo et al., 2013a). AdriaROMS produces hourly output on a regularly spaced 2 km horizontal grid, with 20 generalized terrain following σ-coordinate levels in the vertical. See Russo et al. (2013a,b) for more details about AdriaROMS and Shchepetkin and McWilliams (2005); Haidvogel et al. (2008) for general ROMS setup.

ROMS surface velocities were used to compute offline passive virtual particle trajectories by interpolating velocities to each particle's position and integrating in time using the Matlab ode45 (Runge-Kutta 4/5th order) ordinary differential equation solver. The ROMS domain extended to the 5

m isobath and particles that were advected into shallower areas with no velocity data were fixed at that location for the remainder of the integration (corresponding to stranding).

Following Berta et al. (2014), the ability of ROMS to reproduce observed surface drifter trajectories is assessed by comparing the separation between the virtual particle trajectories and observed CoCoPRO 2013 drifter trajectories

$$D(t) = \sqrt{(x_d - x_p)^2 + (y_d - y_p)^2} \tag{1}$$

with the absolute dispersion (AD) of the drifters

$$AD(t) = \sqrt{(x_d(t) - x_d(0))^2 + (y_d(t) - y_d(0))^2} \tag{2}$$

Here, x and y correspond to position (longitude and latitude) and the subscripts d and p correspond to drifter and particle, respectively. 1000 virtual particles were released within 1 km of daily drifter positions. Particles were tracked for 15 days and reseeded at each new drifter location every 24 hr. $D(t)$ and $AD(t)$ were computed at hourly intervals. The AD provides an indication of the expected uncertainty in virtual particle position over time given no other information (Berta et al., 2014). The separation rate $D(t)$ is quite stringent since it is based on the hindcast of virtual particle trajectories that are chaotic in the sense that they show a high degree of sensitivity to the details of the velocity field (Griffa et al., 2004). In addition to the quantitative $D(t)$ metric, we also compare particle-drifter pathways and transit times.

300 passive virtual particles were released in regions 1-3 and 6-7 every 24 hr beginning 1 May and ending 17 July 2013, for a total of 23100 virtual

particles per region. Particles were not released in regions 4 and 5 because the southern extents of these regions intersected the southern open boundary in AdriaROMS (Fig. 1b). Particles were released in the offshore section of each region to minimize stranding. Particles were tracked for 45 days to permit a sufficient number of particle releases during May–August 2013 to capture the response of surface transport to wind forcing. The 45 day lifetime resulted in 40 releases under variable southerly wind conditions and 31 releases under persistent northwesterly winds (see section 2.7). The 45 day integration time was also chosen with the average drifter-particle separation rate ($D(t)$; eq. 1) in mind. Thus, the 45 day particle lifetime was selected for comparison with the CoCoPro 2013 drifter analysis, to account for model performance, to visualize the impacts of wind variability, and to reflect biologically-relevant time scales.

2.6. Virtual particle transport estimates

The connection percentages and average transit times were computed for virtual particles released in regions 1-3 and regions 6-7. While regions 4 and 5 were not considered as source regions, they were considered as destination regions. The connection percentages for virtual particles were computed in the same manner as for the drifters using the same lifetime limits (in this case L_{30} and L_{45}; see section 2.4). Given the large number of virtual particles released in each region, the mean and standard deviation of the transit time were computed for region pairs. In this case, even a small connection percentage (<1%) corresponds to a relatively large number of connections, especially when compared to drifter results.

2.7. Winds

Surface winds from the numerical weather prediction system COSMO-I7 (Russo et al., 2009; Benetazzo et al., 2013) at 7 km horizontal resolution and hourly temporal resolution were used to assess the influence of the winds on the surface transport as observed by the CoCoPRO 2013 drifters and the virtual particle releases. COSMO is a nonhydrostatic atmospheric model (http://www.cosmo-model.org) developed from the Lokal model described by Steppeler et al. (2003).

The COSMO winds were spatially averaged over the central and southern Adriatic, similar to the averaging employed by Magaldi et al. (2010). See the Appendix for an evaluation of the spatial averaging scheme. Wind regimes are quantified and visualized by computing the direction frequency (wind rose) and a stick plot (Fig. 3). Southeasterly Sirocco and northwesterly Mistral winds are oriented parallel to the coastlines and can strongly influence surface transport both in the boundary currents and in the interior.

3. Results

For the sake of clarity only synthesis-level results are presented in the main body of the text. Supporting information, like confidence intervals for connection percentages, standard deviations of transit times, and histograms of transit times for the L_0, L_{30}, and L_{45} datasets, are shown in the Appendix.

3.1. Drifter transport estimates

Figure 4 presents connection percentages and transit times for the L_0, L_{30}, and L_{45} datasets. The remainder of this subsection is devoted to the results

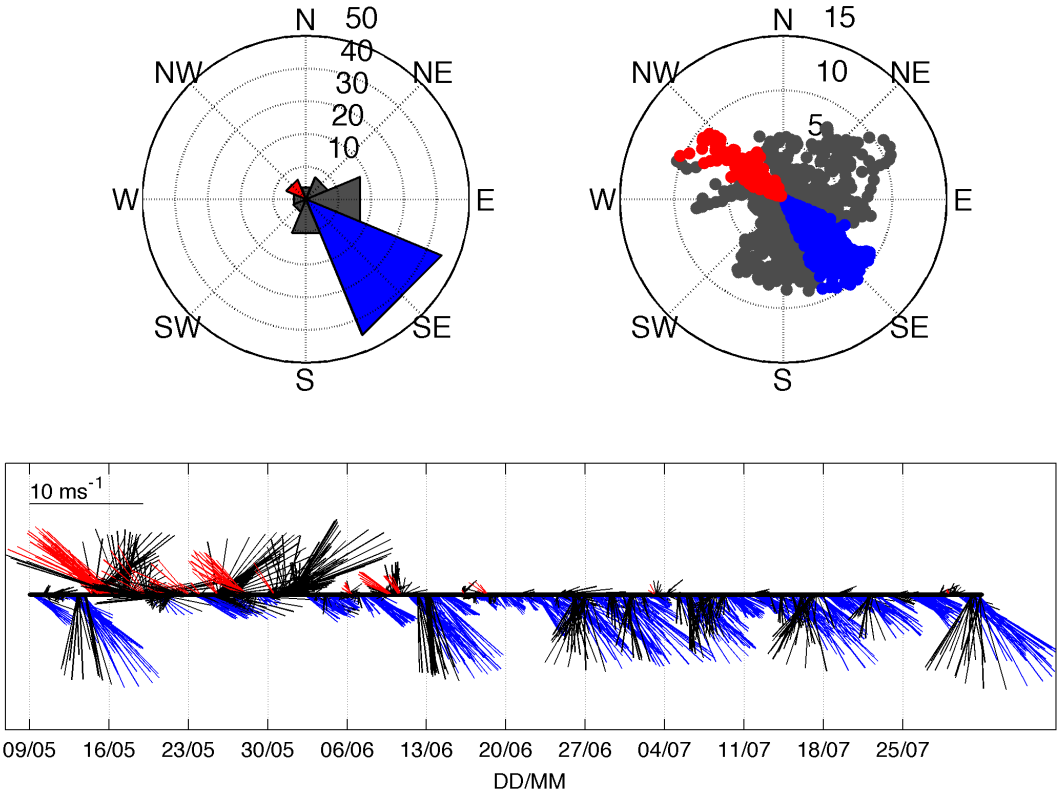

Figure 3: The direction frequency, or wind rose (top left), wind speeds (top right) and stick plot (bottom) of the spatially averaged hourly COSMO winds in the central Adriatic Sea from 10 May to 31 July 2013. Southeasterly and northwesterly wind events are shown in red and blue, respectively. Here, the oceanographic convention shows the direction the wind was blowing towards.

summarized in Figure 4. The L_0 dataset resulted in the largest numbers of drifters available to evaluate transport. Connection percentages were highest for L_0. Average transit times were computed for the 11 region pairs that were connected by at least 10 drifters (see section 2.4). Average transit times were generally relatively short (9-40 days). However, the average transit times between region 7 and regions 1-4 all exceeded 40 days, suggesting that, in the central region, cross-Adriatic transport occurred at longer time scales.

The L_0, L_{30}, and L_{45} datasets reveal the importance of temporal scales in realizing transport between regions. Compared to L_0, both connection percentages and transit times decrease for L_{30}, reflecting the requirement that connections occur within 30 days. When compared to L_{30}, connection percentages and transit times for L_{45} either did not change, or increased. The increase observed for L_{45} results from the fact that drifters had a longer time period over which to realize connections.

Regions 1, 2, 3, 6, and 7 were connected to other central Adriatic destinations in the L_0, L_{30}, and L_{45} datasets, suggesting strong connections between most of the central Adriatic regions that could be realized over a range of time scales. Average transit times ranged from 9–61 days, 7–20 days, and 8–30 days for the L_0, L_{30}, and L_{45} datasets, respectively. In general, alongshore connection percentages were highest from a given source region to a nearby downstream destination. Considering region 1 as the source, the connection percentage for region 2 was highest at all time scales (70%-81%) and appreciable for regions 3 (47%-61%) and 4 (9%-33%). Similar results were observed for downstream, alongshore connections when considering regions 2, 3, 5, and 6 as sources. Alongshore connections were slightly lower on the east coast

though this could result from the spatial distribution of drifter observations (Fig. 2). Small connection percentages from region 2 to region 1 and from region 3 to region 2 suggest that transient southeasterly Sirocco winds are an important driver of upstream connections on the western (Italian) coast.

East-to-west cross-Adriatic connection percentages were higher than west-to-east in the central Adriatic. For example, L_{45} connection percentages from region 6 to regions 1-4 ranged from 8%-15%. Similarly, L_{45} connection percentages from region 7 to regions 1-3 ranged from 12% to 23% while L_{45} connection percentages from regions 1-3 to regions 6 and 7 were several times smaller (2%-4%).

Regions 6 and 7 were connected to region 4 in the southwest Adriatic, with connection percentages of 15% and 12%, respectively for L_{45}. Connection percentages from region 4 to regions 6 and 7 were much smaller (2%). Eastward cross-basin transport in the southern Adriatic was observed from region 4 to region 5, with 4% of drifters leaving region 4 reaching region 5 for L_{45}. The L_{45} dataset shows that drifters from region 5 travelled primarily to regions 6 and 7, with 5% reaching region 2. Region 6 appeared more connected with the west coast in both directions than region 5.

Region-specific transport pathways for the L_{45} dataset are shown in Figure 5. The majority of L_{45} drifters that left regions 1-4 were carried alongshore in the WAC. West-to-east transport was achieved through the northern, central, and southern gyres. Most of the L_{45} drifters that left region 4 exited the Adriatic Sea in the western Otranto Strait. L_{45} drifters that originated from regions 5-7 show the influence of the EAC as well as east-to-west crossings in the three main gyres.

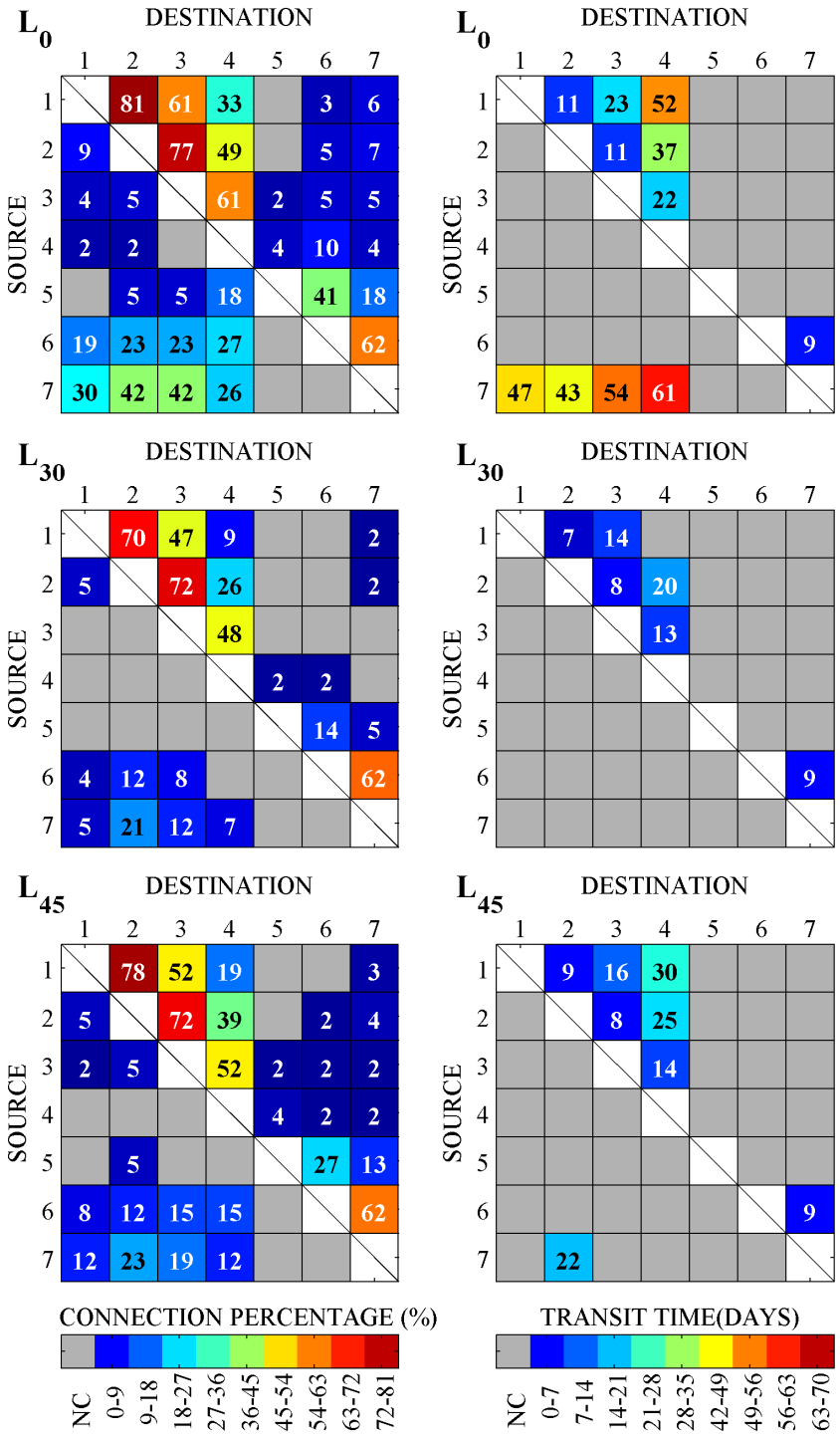

Figure 4: Connection percentages (left column) and average transport times (right column) computed from drifter data for the L_0 dataset (top row), the L_{30} dataset (middle row), and the L_{45} dataset (bottom row). "NC" in the color scales indicates no connection. Confidence intervals for the connection percentages and transit times, as well as histograms of transit times, are shown in the Appendix.

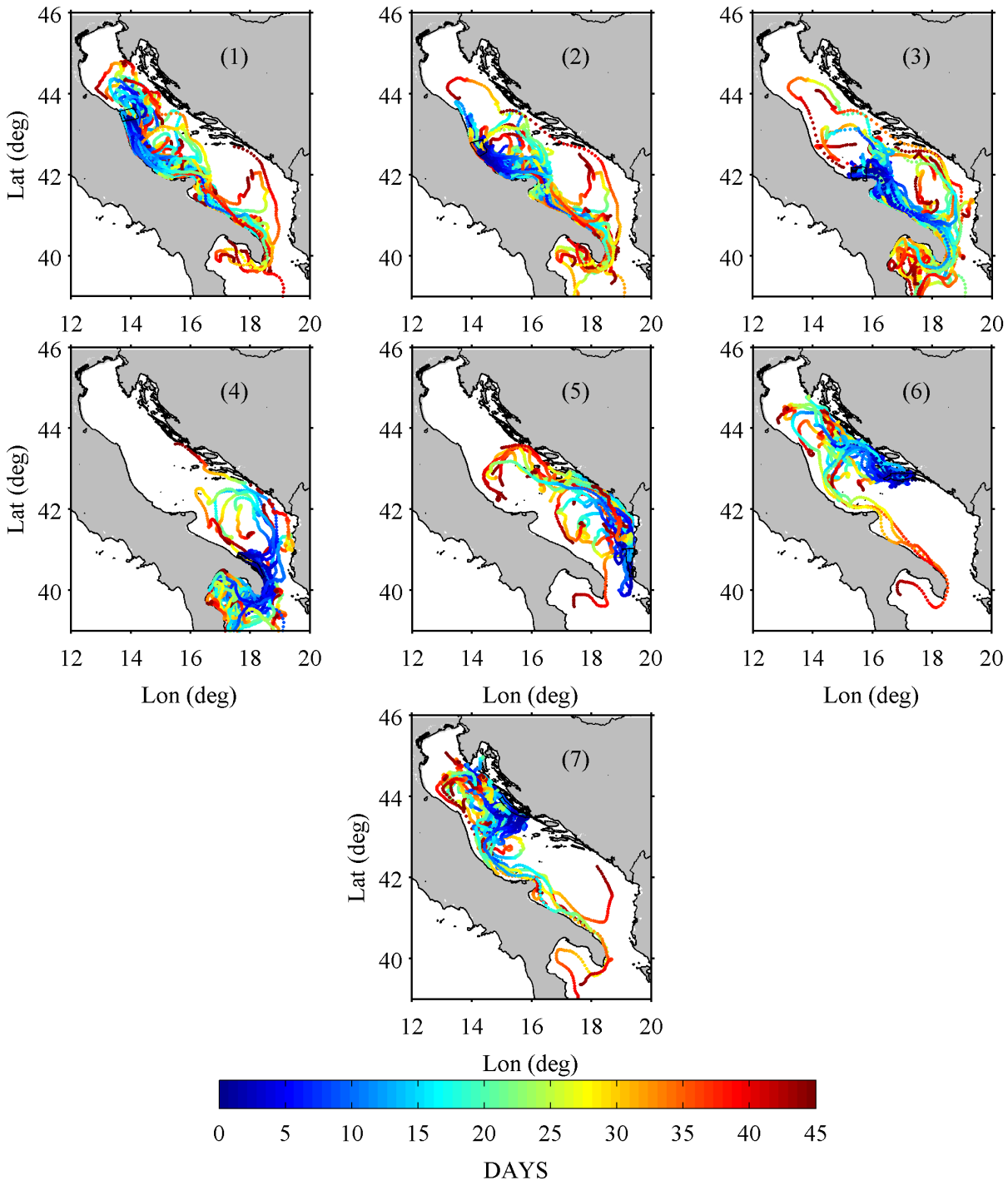

Figure 5: L_{45} drifter trajectories from each source region. Drifter positions are color-coded to indicate time since leaving the source region boundaries. Source region numbers are shown in each panel.

3.2. Wind effects on CoCoPRO 2013 drifters

The CocoPRO 2013 drifters resolved the surface circulation in the central and southern Adriatic Sea at synoptic timescales during early-mid summer (May-July) 2013. Mesoscale, synoptic transport is strongly influenced by the winds and, as a result, we examine variability in the winds during the CoCoPRO 2013 campaign. Northwesterly winds dominated throughout the experiment period though two distinct regimes appear to divide the CoCoPRO experiment period almost in half (Fig. 3a). The first period (8 May to 10 June) was characterized by strong wind speeds (10 ms^{-1}) and variable directions (Fig. 3c). Several southeasterly wind episodes that lasted for one day or longer were observed during the first half of the experiment (Fig. 3c). The second period (10 June to 31 July) was characterized by periods of persistent northwesterly winds (Fig. 3). The transition in June to primarily northwesterly winds agrees with expected seasonal patterns (Bignami et al., 2007; Pasarić et al., 2009; Klaić et al., 2009).

The effects of southeasterly and northwesterly winds on transport pathways was investigated using methods similar to those employed by Ursella et al. (2006) in the northern and central Adriatic Sea. Drifter velocity data at hourly intervals were selected according to the orientation of the basin-averaged winds. Drifter velocities during southeasterly and northwesterly winds were then averaged in 0.25 ^{o} bins to provide indications of circulation and transport patterns induced by a given wind regime. Due to the small number of drifter data, no minimum cut-off on the number of data per bin was considered, so that the resulting velocity fields cannot be regarded as significant averages, but rather as indications of the velocity as sampled along

drifter tracks (Schroeder et al., 2011).

Southeasterly winds are expected to induce Ekman transport away from the Italian coast and toward the Balkan coast, with intensification of the EAC and upwelling on the west coast and weakening in the WAC (Magaldi et al., 2010). Northwesterly winds, on the other hand, are expected to cause Ekman transport toward the Italian peninsula, reinforcing the WAC (Magaldi et al., 2010). The bin-averaged drifter velocity patterns during southeasterly and northwesterly winds (Fig. 6), agree well with these expectations, as well as with previous studies (Burrage et al., 2009; Magaldi et al., 2010; Poulain, 1999, 2001; Poulain et al., 2004). The WAC was enhanced during northwesterly winds (Fig. 6b), and weaker (and even reversed near the Gargano Promontory) during southeasterly winds; the EAC appeared stronger during southeasterly winds (Fig. 6a).

The winds affected the cyclonic sub-gyres and subsequent cross-basin transport. The only west-to-east cross-Adriatic transport observed during the CoCoPro 2013 experiment occurred during May 2013 in response to strong southeasterly winds. Southeasterly winds enhanced transport toward the Balkan coast in both the central and southern gyres, as indicated by the approximately northward currents along 16^o E and 18.5^o E (Fig. 6a).

During northwesterly winds, pathways toward the Italian coast were well marked in both gyres (Fig. 6b). The enhanced transport during southeasterly and northwesterly winds is especially evident when compared to historical averages (see for instance Figure 4 in (Poulain, 1999)). Average velocities computed for each half of the experiment period (i.e. 8 May to 10 June and 10 June to July 31; Figure 6c-d) are qualitatively similar to the

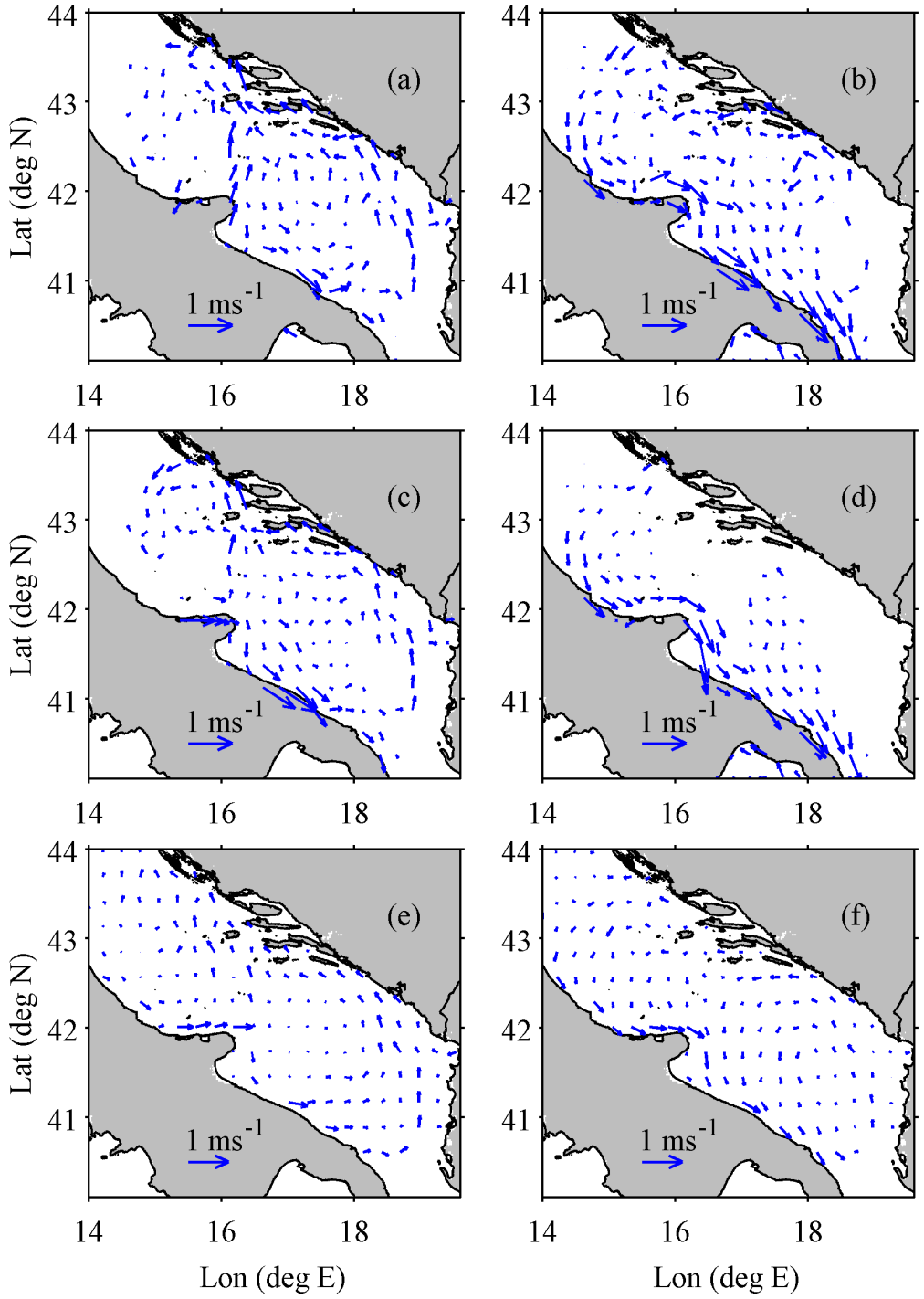

Figure 6: Velocities averaged in 0.25^o bins during (a) southeasterly winds, (b) northwesterly winds, (c) 10 May - 10 June 2013, and (d) 11 June - 31 July 2013. Some bins were located over land, but included nearshore drifter velocities. Panels (e) and (f) show average AdriaROMS surface velocities during southeasterly and northwesterly winds, respectively, during the same period.

velocities averaged according to wind direction, confirming the influence of the southeasterly and northwesterly regimes during first and second halves of the experiment, respectively.

MODIS chlorophyll-a images images obtained before (14 May 2013) and after (20 May 2013) a strong southerly and southeasterly wind event (Fig. 7) illustrate the effect of Sirocco winds on the WAC. At the onset of southerly winds the WAC could be identified as high chl-a band close to the Italian Adriatic coastline, with a sharp offshore front (Fig. 7a). After 6 days of southerly and southeasterly winds the WAC deviated from its typical form with several high chl-a filaments, presumably originating from the west coast of the Adriatic in the WAC, extending eastward across most of the Adriatic (Fig. 7b). One filament extended from the Gargano Promontory northward towards region 6 in the Dalmatian Islands (Fig. 7b), in agreement with the northward velocities observed along 16^o E (Fig. 6a,c). Section 3.4 explores the impacts of wind variability during the CoCoPro 2013 experiment in detail using virtual particles released in the central Adriatic regions.

3.3. CoCoPRO 2013 drifter–ROMS comparison

Comparison of the average and standard deviation of the drifter-virtual particle separations $D(t)$ to the average drifter absolute dispersion $AD(t)$ shows that the average virtual particle position uncertainty was almost the same as the drifter AD at short times (< 1 day) and was smaller than the AD at longer times (Fig. 8a). The large relative uncertainty at short times likely resulted from the effects of unresolved processes (i.e., processes with spatial and/or temporal scales less than the model spatial and temporal resolutions, respectively) on the model's ability to make short-term predictions. At longer

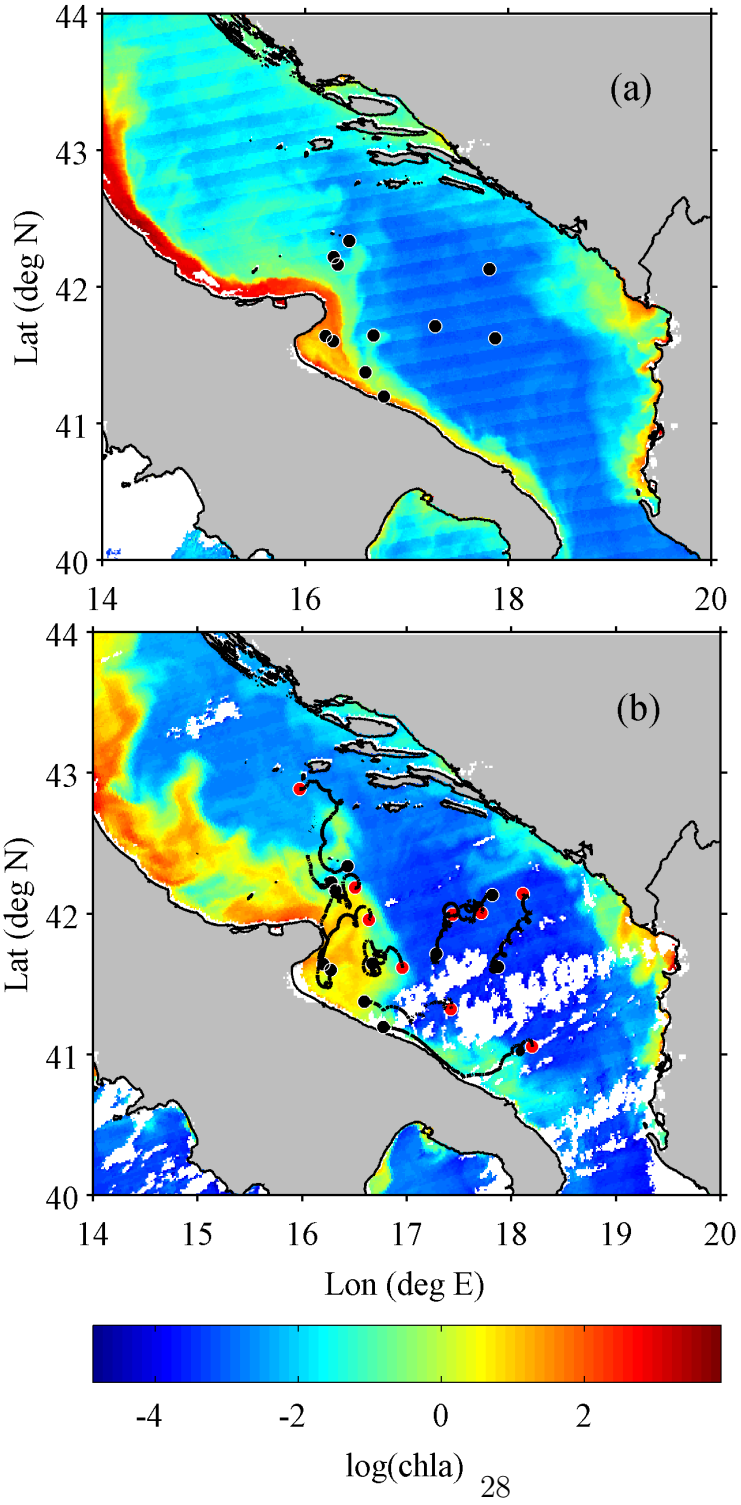

Figure 7: MODIS chlorophyll-a imagery showing conditions from (a) 14 May 2013 before a strong southerly wind event and from (b) 20 May 2013 at the end of the event. In (b) the red circles denote 20 May drifter positions while black circles correspond to drifter positions at 14 May (panel a). The black lines show drifter trajectories during the period 14-20 May

times (8-15 days) the average separation is approximately 75% the average drifter AD (Fig. 8a), suggesting that the model adequately replicates the general circulation features and mesoscale/synoptic-scale phenomena.

The complex topography introduced by the Dalmatian Islands combined with the limited spatial resolution of AdriaROMS made particle tracking near the east coast challenging. The blue trajectory in Figure 8b shows a drifter from the eastern, central Adriatic that progressed northwestward through the Dalmatian Islands of Croatia. A subset of virtual particles (grey trajectories) followed the drifter reasonably well until the Dalmatian Islands. The other subset of virtual particles turned abruptly to the east and later to the south, clearly deviating from the observed drifter trajectory. The green trajectory in Figure 8b shows a drifter that began near the Croatian coast. Virtual particles separated from the drifter in the interior of the Adriatic. The last example in Figure 8b shows a large initial separation between the observed drifter trajectory (in red) and the virtual particles (grey) as the drifter moved offshore and the particles were advected rapidly alongshore in the WAC. Observed drifter trajectories and virtual particle trajectories during the period of persistent northwesterly winds (2–17 June 2013) in general show somewhat better agreement (Fig. 8c).

3.4. Virtual particle trajectories during May–August 2013

Figure 9 shows virtual particle connection percentages and average transit times. In general, the L_{45} connection percentages were larger than L_{30} estimates. Average transit times were also larger for the L_{45} dataset. In the western Adriatic, connection percentages were large (91% - 98%) for adjacent, downstream regions. Average downstream transit times from regions

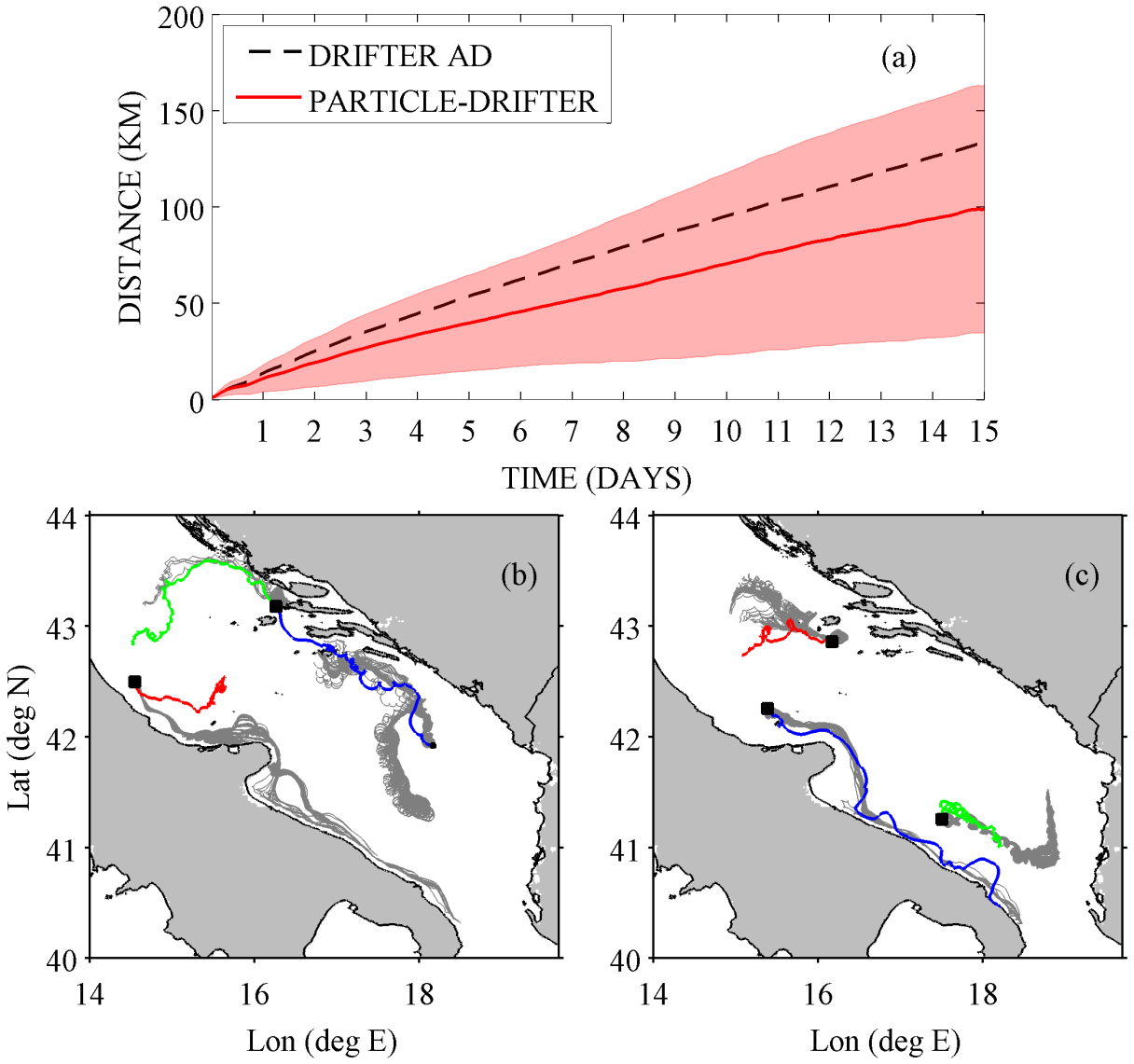

Figure 8: (a): Average (thick red line) and standard deviation (shaded red area) of drifter-particle separation as a function of time. The dashed black line shows the average drifter absolute dispersion as a function of time. (b-c): Observed drifter trajectories (colors) and example virtual trajectories (gray). Trajectories began at the black squares.

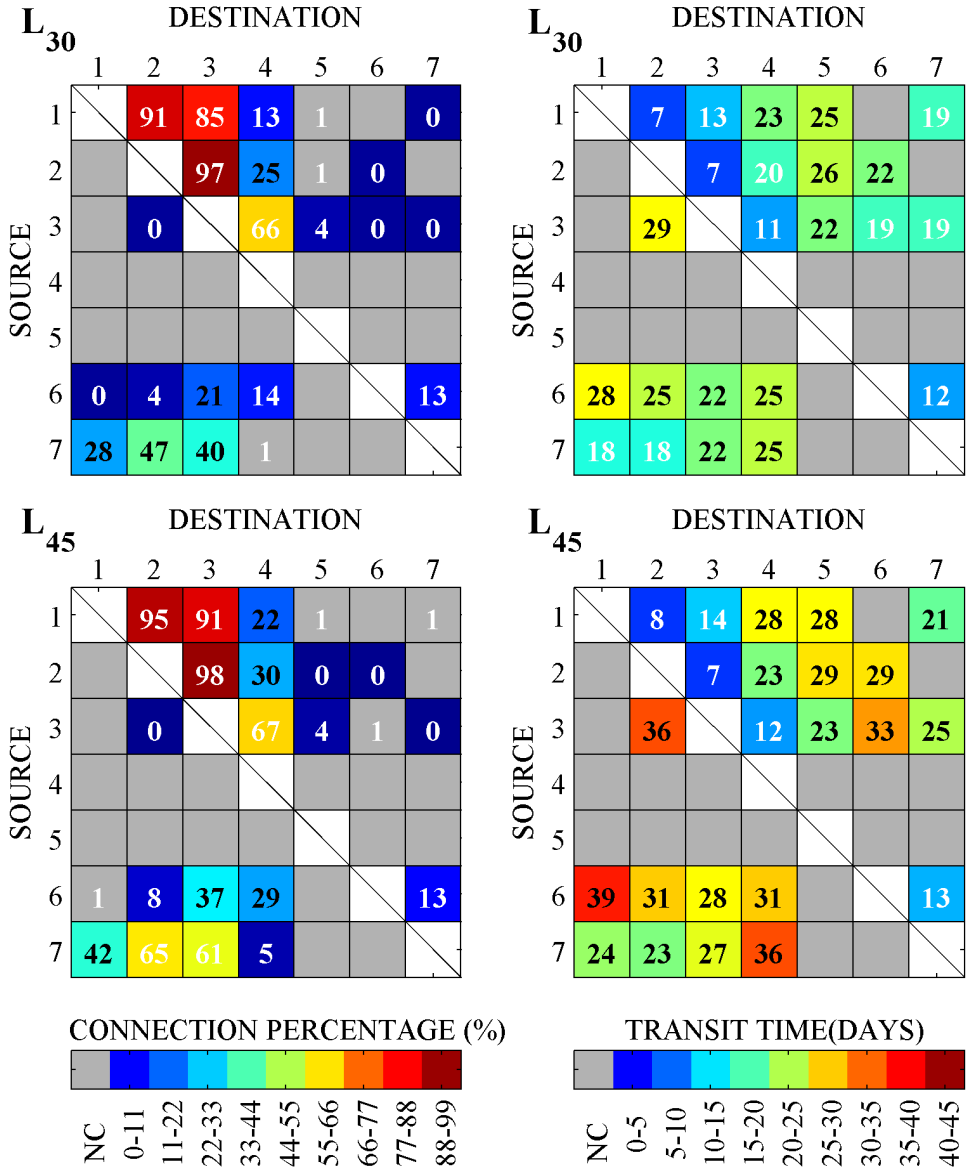

Figure 9: Connection percentages (left column) and average transport times (right column) computed from virtual particle trajectories for the L_{30} dataset (top row) and the L_{45} dataset (bottom row). A connection percentage of 0 denotes an actual percentage that was less than 1%. "NC" in the color scales indicates no connection. Confidence intervals for the connection percentages and standard deviations of the transit times, as well as histograms of transit times, are shown in the Appendix.

1 and 2 to regions 2 and 3 were about 7 days. Region 4 (Torre Guaceto) was most strongly connected (66%) with region 3 (Gargano) with an average transit time of approximately 12 days. Particles originating in regions 1-3 crossed the Adriatic, reaching regions 5-7. The largest eastward cross-Adriatic connection percentages were observed between regions 3 and region 5 (approximately 4%) with average transit times of 22–23 days. Otherwise, transport between regions 1-3 and regions 6-7 was quite limited (<1%) with transit times ranging from 19 days to 29 days. Weak (<1%) upstream connection percentages were observed from region 3 to region 2, with longer average transit times (30 days or more).

On the east coast, the connection percentage for particles leaving region 6 and traveling to region 7 was 13% with average transit times of approximately 12 days. This connection percentage is about 7 times smaller than alongshore, downstream values on the west coast (for example, 95% between regions 1 and 2). Cross-Adriatic transport was higher from east-to-west with strong connections between region 6 and region 3 with an average transit time of approximately 25 days. 47% and 65% of particles seeded in region 7 reached region 2 at lifetime limits of 30 days and 45 days, respectively, with corresponding average transit times of 18 days and 23 days. No upstream transport was observed between regions on the east coast.

Two test cases of particle releases reveal the respective influence of Sirocco and Mistral winds on surface transport pathways. Particles released 15 May (Fig. 10) in regions 1 and 3 rapidly crossed the Adriatic in response to the strong southeasterly and southerly winds observed 14–20 May 2013 (Fig. 3). During this time, particles released in region 2 traveled into the interior of

the Adriatic, but did not reach regions 6 or 7 on the east coast (Fig. 10). Trajectories of particles released in region 3 agree well with the CoCoPRO 2013 drifters deployed in and near region 3 during mid-May 2013 (Fig. 2c) as well as the MODIS chl-a filaments observed after the southeasterly wind event that spanned the period 14–20 May (Fig. 7). Particles from region 6 traveled alongshore (northwestward) in an enhanced EAC and then crossed the Adriatic towards the west coast near regions 2 and 3 (Fig. 10). Some particles from region 7 travelled northwestward in the EAC to the northern Adriatic before crossing the Adriatic in the northern arm of the northern gyre and then traveling southeastward to reach regions 1-3 (Fig. 10) while some particles traversed the central Adriatic via the central gyre.

The persistent northwesterly winds during July 2013 (Fig. 3) resulted in westward transport in the interior and enhanced southeastward transport in the WAC (Fig. 11). Particles from regions 1-3 traveled southeastward in the WAC with no eastward transport observed (Fig. 11). On the east coast, particles from region 6 reached the west coast after 30-45 days while particles released in region 7 took a faster (15–20 days) route across the Adriatic in the northern arm of the central gyre (Fig. 11). Region 6 showed stronger connections with regions 2 and 3 while region 7 was connected with regions 1-3 (Fig. 11).

4. Discussion

We assessed surface transport pathways between coastal regions in the central and southern Adriatic Sea using drifter observations and virtual particle trajectories. The drifter results provide ensemble information of synoptic

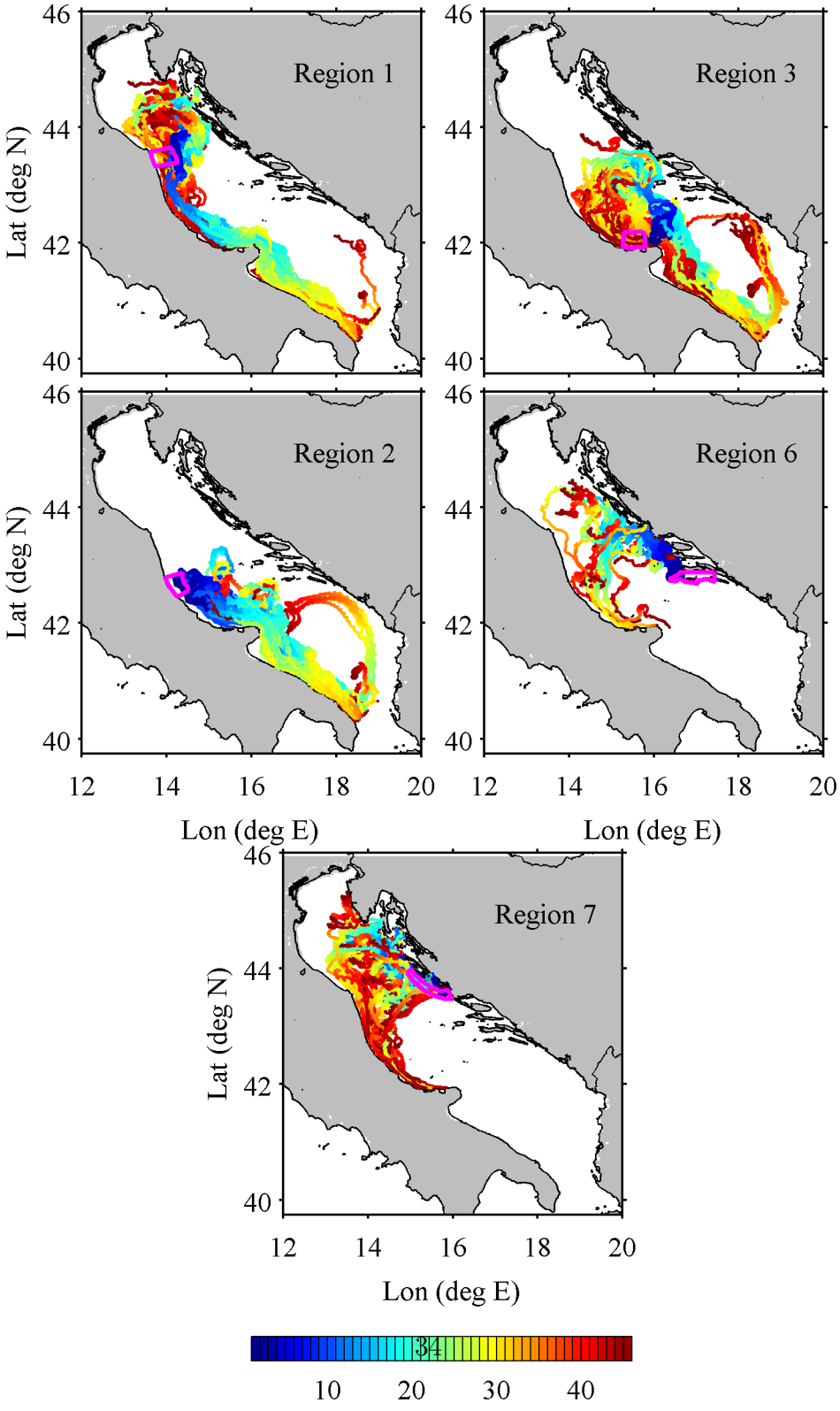

Figure 10: 300 virtual particles were released in regions 1-3 and 6-7 on 15 May 2013 and tracked for 45 days using the ROMS surface velocities. Particle positions are color-coded according to time (in days) since release. Region boundaries are plotted in magenta.

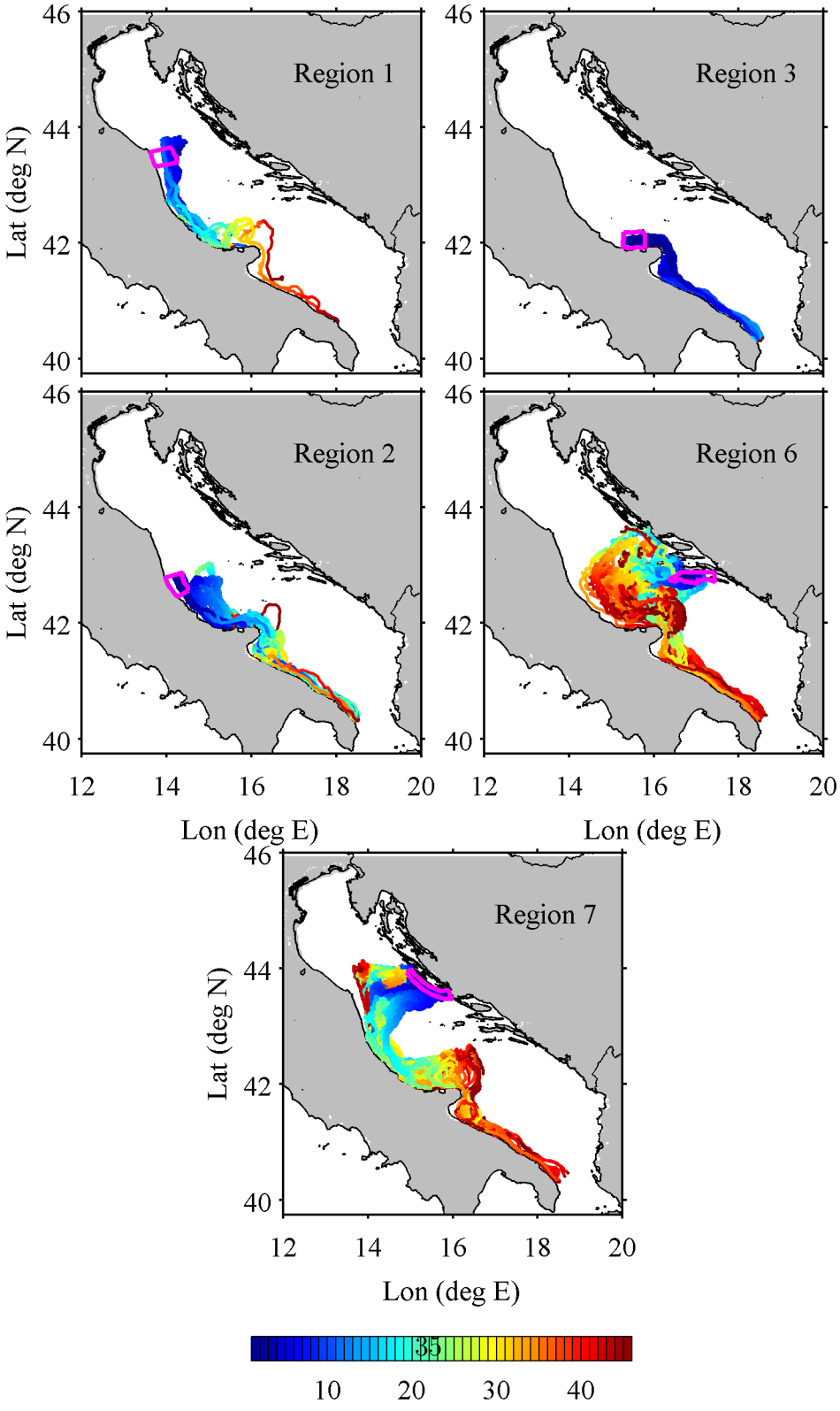

Figure 11: 300 virtual particles were released in regions 1-3 and 6-7 on 1 July 2013 and tracked for 45 days using the ROMS surface velocities. Particle positions are color-coded according to time (in days) since release. Region boundaries are plotted in magenta.

to seasonal surface transport over 25 years. Furthermore, drifter observations represent the cumulative effects of ocean processes from the basin-scale circulation down to variability at the drifter space and time scales (i.e. ˜O(1 m) and ˜O(hr)).

The drifter observations show that the highest connection percentages were achieved for regions connected by the WAC and the EAC in their respective downstream directions (Fig. 4). The highest connection percentage (78%) was observed for transport of drifters from region 1 (Conero) to region 2 (Torre del Cerrano), with an average transit time of 9 days. Similar values were reported for transport of drifters from region 6 (Mljet) to region 7 (Kornati). Upstream alongshore connections were an order of magnitude smaller and were only observed on the western (Italian) coast, presumably due to wind-driven WAC reversals. When considered as a destination, region 4 (Torre Guaceto) was strongly connected with region 3 (Gargano) with a connection percentage of 52% and an average transit time of 13 days. The WAC connected regions 1 and 2 with region 4 with average transit times of 30 days and 25 days, respectively.

As the Torre Guaceto MPA has been presented as a successful model of resource management in the Adriatic Sea, the results for region 4 could be of particular interest to ecologists given the relatively strong connection percentages (20-40%) and ecologically relevant transit times. Region 5 (Karaburun) also deserves attention as it encompasses the lone MPA in the southeast Adriatic. Relatively few drifters entered Region 5 and those that did show that it acted mainly as a source, with 27% of drifters leaving region 5 traveling to region 6. When considered as a destination, connection percentages

were an order of magnitude lower. Transit time estimates for region 5 are not available.

Virtual particle trajectories allow detailed investigations of specific events, like a strong southeasterly Sirocco wind event, using a large number of particles. While the large number of virtual particles allowed computation of robust statistical estimates, the resolution of the underlying Eulerian velocities (Haza et al., 2007; Putman and He, 2015) affected the particle trajectories. Putman and He (2015) stress the importance of resolution in modeling marine connectivity, as well as the importance of drifter-based model validations. Thus, our analysis is completed by a validation of the virtual trajectories computed from AdriaROMS surface velocity fields. The ROMS velocities were computed over a high resolution ($\frac{1}{45}^o$) horizontal grid, yet particle-drifter separation rates of 5-6 km day^{-1} (Fig. 8a) reveal the importance of unresolved, sub-grid-scale processes even in a high resolution model. Separations of this magnitude are not uncommon in particle tracking studies (Liu and Weisberg, 2011; Putman and He, 2015) though the impacts of these separations on the accuracy of transport and connectivity estimates have yet to be determined. In this particular study, the relatively small drifter-model separation and the qualitative agreement of virtual particle trajectories with observed chl-a distributions (Fig. 7) suggest that AdriaROMS can be used to study transport at synoptic to seasonal time scales.

Qualitative comparisons of CoCoPro 2013 drifter trajectories and virtual particle trajectories (Fig. 8b) highlighted challenges in modeling alongshore trajectories in the eastern Adriatic due to the numerous small islands and narrow channels that were not resolved in the AdriaROMS simulations. The

complex topography was likely responsible for the relatively low connection percentage between region 6 and region 7 in the Dalmatian Islands. For example, the drifter observations show a connection percentage of 62% from region 6 to region 7 with an average transit time of 9 days (Fig. 4). The virtual particle results, on the other hand, show connection percentages that are 5 times smaller (13%) with slightly longer average transit times of 12 and 13 days. The smaller connection percentage and the longer transit time likely reflect the fact that virtual particles could not take a direct route nearshore and the connection was, instead, realized by particles that took a longer route offshore.

While the topography in the western Adriatic is simple when compared to the eastern Adriatic, the 5 m minimum depth in AdriaROMS means that transport in the shallow coastal boundary layer was not resolved, especially in areas with a gentle bottom slope. Given that across-shore transit through the coastal boundary layer can take days (Largier, 2003), the transit times in Figure 9 are likely biased towards shorter times.

Drifter observations and virtual particle trajectories suggest that east-to-west transport was stronger than west-to-east, in agreement with previous studies (Poulain, 2001; Vilibić et al., 2009). Eastward transport of western Adriatic waters occurs irregularly and has been linked to variability in wind forcing (Bignami et al., 2007; Burrage et al., 2009; Poulain et al., 2004; Vilibić et al., 2009). Extensive eastward transport of WAC waters in response to strong southeasterly and southerly winds that persisted over a 5-day period in May 2013 was documented by surface drifters, virtual particles, MODIS chl-a imagery, and average surface velocities from the ROMS simulation during the

CoCoPro 2013 experiment. Southeasterly winds, however, do not always lead extensive cross-Adriatic transport of western Adriatic waters (Bignami et al., 2007). Vilibić et al. (2009) showed that eastward transport is affected by a combination of winds, topography, coastline geometry, and river discharge, making predictions of easterly transport challenging.

The intensification of the WAC in response to the persistent northwesterly Mistral winds during the second half of the CoCoPro 2013 experiment (July–August 2013) agrees well with previous studies (Bignami et al., 2007; Burrage et al., 2009; Vilibić et al., 2009; Magaldi et al., 2010). More importantly, the observed export of CoCoPro 2013 surface drifters to the northern Ionian Sea (Fig. 2d) and the accumulation of virtual particles at the southwestern boundary of the AdriaROMS domain (Fig. 11) suggests the possibility of connections between central Adriatic regions with MPAs in the northern Ionian Sea.

As the mean flow in the central region favors transport from the eastern Adriatic (regions 6 and 7) towards the western Adriatic (regions 1-3), easterly transport can also be viewed as a disruption of expected transport patterns. Intermittent eastward transport of WAC waters, therefore, could potentially displace organisms out of a suitable environment or, at the very least, decrease the extent of their alongshore transport.

Qualitative comparison of drifter results (Fig. 4) with virtual particle results (Fig. 9) shows remarkable agreement between the estimated transit times and patterns of connection, with two exceptions. First, particle-based connection percentages are lower on the east coast when compared to drifter-based results, as discussed above. Second, connection percentages between

region 7 and regions 1-4 are significantly higher for virtual particles (28-48% for L_{30} in Fig. 9) than for drifters (5-21% in Fig. 4). The drifter results are based on an ensemble average over 25 years (1990-2015) while the virtual particle results are based on three months of simulations and this inherent difference limits our capacity for direct comparison between the two sets of results.

Finally, persistent Lagrangian pathways between regions and MPAs are not always beneficial, especially given the high coastal population density in the Adriatic Sea and the subsequent risk of spills and other anthropogenic catastrophes. For example, the central and southern Adriatic Sea suffers from high abundances of buoyant anthropogenic marine debris (Suaria and Aliani, 2014) and the surface transport pathways identified have as much potential to realize exchange of debris as they do larvae and propagules. Thus, the design of networks of MPAs should not only consider Lagrangian transport pathways, but also the potential for cross-contamination through transport of marine debris/pollutants.

5. Summary and conclusion

Drifter observations and virtual particle trajectories are used to quantify transport between coastal regions at different time scales and to investigate the influence of wind forcing on cross-basin transport. The drifter results suggest that westward cross-Adriatic transport occurred more often than eastward transport. When considering regions 6 and 7 as sources, connection percentages with regions 1-4 were ˜O(10%). Transport from region 7 to region 2 took an average of 22 days. Eastward connection percentages from

regions 1-4 to regions 6-7 were an order of magnitude smaller. As the average surface circulation favors westward transport, the eastward transport events were likely driven by intermittent southeasterly winds.

The importance of the WAC in realizing transport between adjacent, downstream regions is again evident in the virtual particle results, with 98% of particles originating in region 2 reaching region 3 with a corresponding average transit time of 7 days. The corresponding role of the EAC in the eastern Adriatic is difficult to assess due to the inability of the model to resolve the complex topography on the east coast (see section 4). With that limitation in mind, 13% of the particles originating in region 6 reached region 7 with an average transit time of 13 days. The virtual particle results also show stronger westward transport. Region 7 exported significant numbers of particles to regions 1-3 with average transit times of approximately 25 days. Eastward transport was much weaker (1% or less) though average transit times were comparable to their westward counterparts.

The qualitative comparison of trajectories during Sirocco (Fig. 10) and Mistral (Fig. 11) conditions highlight the influence of variable winds on surface transport pathways. During Sirocco winds, particles released in regions 1 and 3 reached the east coast. The trajectories suggest, however, that many of these particles reached coastal areas north of regions 6 and 7. Particles released in region 2 traveled into the interior of the Adriatic but did not reach the east coast. A small number of particles released in regions 1-3 crossed at the Otranto Strait. Particles released in regions 6 and 7 during the Sirocco event traveled north, with some reaching the Istrian peninsula, before crossing to the west coast. Mistral winds enhanced the WAC and re-

sulted in strong downstream connections between regions 1-3. Mistral winds also limited the northward extent of particles released in regions 6 and 7, with faster westward transport observed. Eastward transport during the May 2013 Sirocco event was independently verified using MODIS chl-a imagery (Fig. 7).

In conclusion, the drifter and virtual particle results reveal the importance of the WAC, the EAC, and the gyres in connecting coastal regions in the central and southern Adriatic Sea. The mean cyclonic circulation favors alongshore connections and westward cross-Adriatic transport via the northern arms of the central and southern Adriatic gyres. Eastward transport results primarily from southeasterly Sirocco winds. The partial validation of the AdriaROMS model with the CoCoPro 2013 drifter data suggest that the model performs reasonably well in the central and western Adriatic. While these results represent a critical first step towards evaluating the role of hydrodynamics in connecting MPAs in the Adriatic Sea, dispersal and recruitment occur in three dimensions, close to shore, and are, therefore, affected by turbulent, small-scale features that were not resolved either by the drifters or the AdriaROMS model. Consequently, future studies of hydrodynamic connectivity in the Adriatic Sea should combine non-hydrostatic, high-resolution nested models to compute three dimensional particle trajectories with targeted drifter deployments within MPA boundaries.

Acknowledgements

The authors gratefully acknowledge support from the EU CoCoNET project (FP7, Grant Agreement 287844), the Italian flagship project RIT-

MARE, the Italian national project S.S.D. PESCA, the Ministero dell'Istruzione, dell'Università e della Ricerca, and the SALVE project, funded by OGS in the framework of the ARGO-ITALY action. COSMO-I7 winds were kindly provided by Dr. Tiziana Paccagnella and Ing. Andrea Valentini of Hydro-Meteo-Clima Service (SIMC) of Emilia-Romagna Region Environmental Agency (ARPA-EMR, Bologna, Italy). This research paper is made possible, in part, by a grant from BP/The Gulf of Mexico Research Initiative. Thanks to M. Menna, R. Gerin, and A. Bussani for their help with the drifter data processing.

References

Agresti A, Coull B (1998) Approximate is better than 'exact' for interval estimation of binomial proportions. The American Statistician 52:119–126.

Andrello M, Mouillot D, Beuvier J, Albouy C, Thuiller W, et al. (2013) Low connectivity between Mediterranean marine protected areas: a biophysical modeling approach for the dusky grouper *Epinephelus marginatus*. PLoS ONE 8(7): e68564. doi:10.1371/journal.pone.0068564

Benetazzo A, Carniel S, Sclavo M, Bergamasco A (2013) Wave–current interaction: Effect on the wave field in a semi-enclosed basin. Ocean Modelling. 70: 152–165.

Berline L, Rammou A-M, Doglioli A, Molcard A, Petrenko A (2014) A connectivity-based eco-regionalization method of the Mediterranean Sea. PLoS ONE 9(11):e111978. doi:10.1371/journal.pone.0111978

Berta M, Bellomo L, Magaldi MG, Griffa A, Molcard A, Marmain J, Borghini M, Taillandier V (2014) Estimating Lagrangian transport blending drifters with HF radar data and models: Results from the TOSCA experiment in the Ligurian Current (North Western Mediterranean Sea). Progress in Oceanography. 128: 15–29. doi:10.1016/j.pocean.2014.08.004

Burrage D, Book J, Martin P (2009) Eddies and filaments of the western Adriatic current near Cape Gargano: Analysis and prediction. Journal of Marine Systems 78: S205–S226.

Bussotti S, Guidetti P (2011) Timing and habitat preferences for settlement of juvenile fishes in the marine protected area of Torre Guaceto (South-Eastern Italy, Adriatic Sea). Italian Journal of Zoology 78: 243–254.

Bignami F, Sciarra R, Carniel S, Santoleri R (2007) Variability of Adriatic Sea coastal turbid waters from SeaWiFS imagery. Journal of Geophysical Research 112, C03S10, doi:10.1029/2006JC003518

Cowen RK, Gawarkiewicz G, Pineda J, Thorrold SR, Werner F (2007) Population connectivity in marine systems an overview. Oceanography 20:14–21

Corell H, Moksnes P-O, Engqvist A, Döös K, Jonsson PR (2012) Depth distribution of larvae critically affects their dispersal and the efficiency of marine protected areas. Marine Ecology Progress Series 467:29–46 doi:10.3354/meps09963

Cushman-Roisin B, Korotenko KA, Galos CE, Dietrich DE (2007) Simulation and characterization of the Adriatic Sea mesoscale variability. Journal of Geophysical Research doi:10.1029/2006JC003515.

Davis RE (1985) Drifter observations of coastal surface currents during CODE: The statistical and dynamical views. Journal of Geophysical Research 90: 4756–4772.

Di Franco A, Coppini G, Pujolar JM, De Leo GA, Gatto M, et al. (2012a) Assessing dispersal patterns of fish propagules from an effective Mediterranean marine protected area. PloS ONE 7(12): e52108. doi:10.1371/journal.pone.0052108

Di Franco A, Gillanders BM, De Benedetto G, Pennetta A, De Leo GA, et al. (2012b) Dispersal patterns of coastal fish: implications for designing networks of marine protected areas. PloS ONE 7(2): e31681. doi:10.1371/journal.pone.0031681

Efron B, Tibshirani R (1986) Bootstrap methods for standard errors, confidence intervals, and other measures of statistical accuracy. Statistical Science 1:54–77.

Falco P, Griffa A, Poulain P-M, Zambianchi E (2000) Transport properties in the Adriatic Sea as deduced from drifter data. Journal of Physical Oceanography 30: 2055–2071.

Fenberg PB, Caselle J, Claudet J, Clemence M, Gaines S et al. (2012) The science of European marine reserves: status, efficacy, and needs. Marine Policy 36(5):1012-1021. doi:10.1016/j.marpol.2012.02.021

Gaines SD, Gaylord B, Gerber LR, Hastings A, Kinlan BP (2007) Connecting places: The ecological consequences of dispersal in the sea. Oceanography 20:90–99.

Gawarkiewicz G, Monismith S, Largier J (2007) Observing larval transport processes affecting population connectivity: Progress and challenges. Oceanography 20:40–53.

Griffa A, Piterbarg LI, Özgökmen T (2004) Predictability of Lagrangian particle trajectories: effects of uncertainty in the underlying Eulerian flow. Journal of Marine Research 62:1–35.

Haidvogel DB, Arango H, Budgell WP, Cornuelle BD, Curchitser E, Di Lorenzo E, Fennel K, Geyer WR, Hermann AJ, Lanerolle L, Levin J, McWilliams JC, Miller AJ, Moore AM, Powell TM, Shchepetkin AF, Sherwood CR, Signell RP, Warner JC, Wilkin J (2008) Ocean forecasting in terrain-following coordinates: Formulation and skill assessment of the Regional Ocean Modeling System. Journal of Computational Physics 227:3595–3624.

Hare JA, Churchill JH, RK Cowen, Berger TJ, Cornillon PC, Dragos P, Glenn SM, Govoni JJ, Lee TN (2002) Routes and rates of larval fish transport from the southeast to the northeast United States continental shelf. Limnology and Oceanography 47:1774–1789.

Haza AC, Griffa A, Martin P, Molcard A, Özgökmen TM, Poje AC, Barbanti R, Book JW, Poulain PM, Rixen M, Zanasca P (2007) Model-based directed drifter launches in the Adriatic Sea: Results from the DART experiment. Geophysical Research Letters doi:10.1029/2007GL029634

Klaić ZB, Pasarić Z, Tudor M (2009) On the interplay between sea-land

breezes and Etesian winds over the Adriatic. Journal of Marine Systems. doi:10.1016/j.marsys.2009.01.016

Langård L, Skaret G, Jensen KH, Johannessen A, Slotte A, Nøttestad L, Fernö (2015) Tracking individual herring within a semi-enclosed coastal marine ecosystem: 3-dimensional dynamics from pre- to post-spawning. Marine Ecology Progress Series. doi:10.3354/meps11065.

Largier JL (2003) Considerations in estimating larval dispersal distances from oceanographic data. Ecological Applications 13:S71-S89.

Liu Y, Weisberg RH (2001) Evaluation of trajectory modeling in different dynamic regions using normalized cumulative Lagrangian separation. Journal of Geophysical Research doi:10.1029/2010JC006837

Lugo-Fernández A, Deslarzes KJP, Price JM, Boland GS, Morin MV (2001) Inferring probable dispersal of Flower Garden Banks larvae (Gulf of Mexico) using observed and simulated drifter trajectories. Continental Shelf Research 21:47-67.

Magaldi MG, Özgökmen TM, Griffa A, Rixen M (2010) On the response of a turbulent coastal buoyant current to wind events: the case of the western Adriatic current. Ocean Dynamics 60: 93–122.

Maurizi A, Griffa A, Poulain P-M, Tampieri F (2004) Lagrangian turbulence in the Adriatic Sea as computed from drifter data: Effects of inhomogeneity and nonstationarity. Journal of Geophysical Research. doi:10.1029/2003JC002119

Orlić M, Kuzmić M, Pasarić Z (1994) Response of the Adriatic Sea to the Bora and Sirocco forcing. Continental Shelf Research 14: 91–116.

Pasarić Z, Belušić D, Chiggiato J (2009) Orographic effects on meteorological fields over the Adriatic from different models. Journal of Marine Systems 78: S90–S100.

Pasarić Z, Belušić D, Klaić ZB (2007) Orographic influences on the Adriatic Sirocco wind. In: Annales Geophysicae. Copernicus GmbH, volume 25, pp. 1263–1267.

Paschini E, Artegiani A, Pinardi N (1993) The mesoscale eddy field of the middle Adriatic Sea during fall 1988. Deep Sea Research 40:1365–1377.

Pineda J, Hare JA, Sponaugle Su (2007) Larval transport and dispersal in the coastal ocean: Consequences for population connectivity. Oceanography 20:22–39.

Poulain P-M (1999) Drifter observations of surface circulation in the Adriatic Sea between December 1994 and March 1996. Journal of Marine Systems 20: 231–253.

Poulain P-M (2001) Adriatic Sea surface circulation as derived from drifter data between 1990 and 1999. Journal of Marine Systems 29: 3–32.

Poulain P-M, S Hariri (2013) Transit times and residence times in the Adriatic Sea surface as derived from drifter data and Lagrangian numerical simulations. Ocean Science 9: 713–720. doi:10.5194/os-9-713-2013.

Poulain P-M, Mauri E, Ursella L (2004) Unusual upwelling event and current reversal off the Italian Adriatic coast in summer 2003. Geophysical Research Letters. doi:10.1029/2003GL019121.

Puckett BJ, Eggleston DB, Kerr PC, Luettich Jr RA (2014) Larval dispersal and population connectivity among a network of marine reserves. Fisheries Oceanography doi:10.1111/fog.12067.

Pujolar JM, Schiavina M, Di Franco A, Meli P, Guidetti P, et al. (2013) Understanding the effectiveness of marine protected areas using genetic connectivity patterns and Lagrangian simulations. Diversity and Distributions. 19: 1531–1542. doi:10.1111/ddi.12114

Putman NF, He R (2015) Tracking the long-distance dispersal of marine organisms: sensitivity to model resolution. Journal of the Royal Society Interface doi:10.1098/rsif.2012.0979

Rossi V, Ser-Giacomi E, López C, Hernández-García E (2014) Hydrodynamic provinces and oceanic connectivity from a transport network help designing marine reserves. Geophysical Research Letters 41: 2883–2891. doi:10.1002/2014GL059540

Russo A, Coluccelli A, Iermano I, Falcieri F, Ravaioli M, et al. (2009) An operational system for forecasting hypoxic events in the northern Adriatic Sea. Geofizika 26: 191–213.

Russo A, Coluccelli A, Carniel S, Benetazzo A, Valentini A, Paccagnella T, Ravaioli M, Bortoluzzi G (2013a) Operational models hierarchy for short

term marine predictions: the Adriatic Sea example. In: OCEANS-Bergen, 2013 MTS/IEEE (pp. 1–6)

Russo A, Carniel S, A Benetazzo (2013b) Support for ICZM and MSP in the Adriatic Sea region. Sea Technology 54:27–35.

Schroeder K, Haza A, Griffa A, Özgökmen TM, Poulain P-M, et al. (2011) Relative dispersion in the Liguro-Provencal basin: From sub-mesoscale to mesoscale. Deep Sea Research Part I: Oceanographic Research Papers 58: 209–228.

Shanks AL (2009) Pelagic larval duration and dispersal distance revisited. The Biological Bulletin 216: 373–385.

Shchepetkin AF, McWilliams JC (2005) The regional ocean modeling system (ROMS): a split-explicit, free-surface, topography-following-coordinate oceanic model. Ocean Modelling 9:347–404. doi:10.1016/j.ocemod.2004.08.002

Steppeler J, Doms G, Schättler U, Bitzer H, Gassmann A, et al. (2003) Meso-gamma scale forecasts using the nonhydrostatic model lm. Meteorology and Atmospheric Physics 82: 75–96.

Suaria G, Aliani S (2014) Floating debris in the Mediterranean Sea. Marine Pollution Bulletin 86 (1): 494–504.

Tang L, Sheng J, Hatcher BG, Sale PF (2006) Numerical study of circulation, dispersion, and hydrodynamic connectivity of surface waters on the Belize shelf. Journal of Geophysical Research doi:10.1029/2005JC002930

Tilburg CE, Houser LT, Steppe CN, Garvine RW, Epifanio CE (2006) Effects of coastal transport on larval patches: Models and observations. Estuarine Coastal and Shelf Science 67:145–160. doi:10.1016/j.ecss.2005.11.019

Treml EA, Halpin PN, Urban DL, Pratson LF (2008) Modeling population connectivity by ocean currents, a graph-theoretic approach for marine conservation. Landscape Ecology 23:19–36. doi:10.1007/s10980-007-9138-y

Ursella L, Poulain P-M, Signell RP (2006) Surface drifter derived circulation in the northern and middle Adriatic Sea: Response to wind regime and season. Journal of Geophysical Research. doi:10.1029/2005JC003177.

Vilibić I, Book JW, Paklar GB, Orlić M, Dadić V, Tudor M, Martin PJ, Pasarić M, Grbec B, Matić F, Mihanović H, Morović M (2009) West Adriatic coastal water excursions into the East Adriatic. Journal of Marine Systems. 78:S132–S156. doi:10.1016/j.jmarsys.2009.01.015

Appendix A. Supporting Information

Supporting information for results presented in section 3 is presented here for the interested reader.

The complex (vector) correlation between the spatially averaged wind vectors and the wind vector at each COSMO grid-point over the Adriatic Sea was computed from May to July 2013, corresponding to the CoCoPRO 2013 drifter experiment. The correlation coefficients exceed 0.8 over most of the Adriatic Sea (Fig. A.12a), and the phase difference (Fig. A.12b) between the vectors is rather small (within a few degrees), indicating that the averaging domain is appropriate.

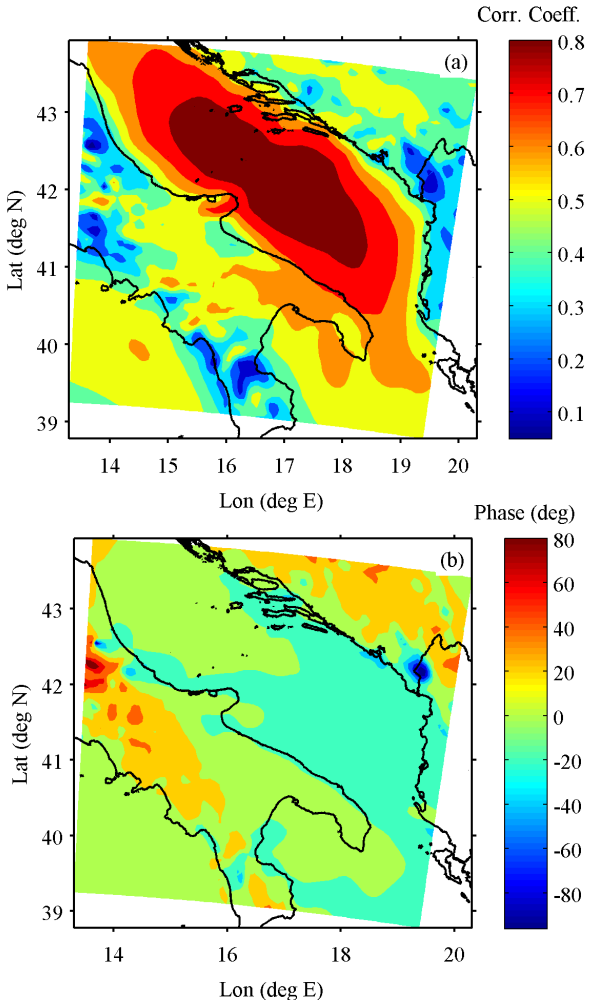

Figure A.12: The complex correlation between the average wind vector components with the 7 km COSMO winds over the central Adriatic Sea shows that the correlation coefficient (a) exceeds 0.8 over most of the Adriatic Sea and that the phase difference (b) between the vectors is rather small (within a few degrees) over the Adriatic Sea.

The connection percentages and transit times in Figures 4 and 9 are based on the results of the tables below. These tables show the total number of drifters that entered a source region, the connection percentage between source region and destination region and 95% confidence intervals computed using the Wilson score. Tables A.1-A.3 summarize results from the drifter datasets. Tables A.4-A.5 show results based on the virtual particle trajectories. Histograms of drifter-based transit times are shown in Figures A.13-A.16 while transit times of virtual particles are shown in Figures A.17-A.18.

SRC = 1	ND = 64			SRC = 2	ND = 57		
DST	%	LB	UB	DST	%	LB	UB
2	79.68	68.28	87.72	1	3.50	0.96	11.92
3	60.93	48.69	71.94	3	77.19	64.79	86.15
4	32.81	22.57	45.00	4	49.12	36.61	61.74
5	-	-	-	5	-	-	-
6	3.12	0.86	10.69	6	5.26	1.80	14.36
7	4.68	1.60	12.89	7	7.01	2.76	16.70
SRC = 3	ND = 56			SRC = 4	ND = 50		
DST	%	LB	UB	DST	%	LB	UB
1	-	-	-	1	2	0.35	10.49
2	-	-	-	2	2	0.35	10.49
4	60.71	47.63	72.41	3	-	-	-
5	1.78	0.31	9.44	5	4	1.10	13.46
6	5.35	1.83	14.60	6	10	4.34	21.36
7	5.35	1.83	14.60	7	4	1.10	13.46
SRC = 5	ND = 22			SRC = 6	ND = 26		
DST	%	LB	UB	DST	%	LB	UB
1	-	-	-	1	15.38	6.14	33.53
2	4.54	0.80	21.79	2	23.07	11.03	42.05
3	4.54	0.80	21.79	3	19.23	8.50	37.87
4	13.63	4.74	33.33	4	26.92	13.70	46.08
6	40.90	23.25	61.26	5	-	-	-
7	18.18	7.30	38.51	7	61.53	42.53	77.57
SRC = 7	ND = 43						
DST	%	LB	UB				
1	27.90	16.74	42.69	-	-	-	-
2	41.86	28.38	56.67	-	-	-	-
3	39.53	26.36	54.42	-	-	-	-
4	25.58	14.92	40.23	-	-	-	-
5	-	-	-	-	-	-	-
6	-	-	-	-	-	-	-

Table A.1: L_0 drifter results with the number of drifters leaving a given source (SRC) region indicated as ND. The connection percentage (%) quantifies the percentage of ND that reached a given destination region (DST). The Wilson Score estimates the upper (UB) and lower bounds (LB) for each connection percentage. A dash '-' indicates no connection between source and destination.

SRC = 1	ND = 64			SRC = 2	ND = 57		
DST	%	LB	UB	DST	%	LB	UB
2	70.31	58.22	80.09	1	5.26	1.80	14.36
3	46.87	35.17	58.92	3	71.92	59.16	81.92
4	9.37	4.36	18.98	4	26.31	16.64	38.97
5	-	-	-	5	-	-	-
6	-	-	-	6	-	-	-
7	1.56	0.27	8.33	7	1.75	0.31	9.29
SRC = 3	ND = 56			SRC = 4	ND = 50		
DST	%	LB	UB	DST	%	LB	UB
1	-	-	-	1	-	-	-
2	-	-	-	2	-	-	-
4	48.21	35.66	60.98	3	-	-	-
5	-	-	-	5	2	0.35	10.49
6	-	-	-	6	2	0.35	10.49
7	-	-	-	7	-	-	-
SRC = 5	ND = 22			SRC = 6	ND = 26		
DST	%	LB	UB	DST	%	LB	UB
1	-	-	-	1	3.84	0.68	18.89
2	-	-	-	2	11.53	4.00	28.97
3	-	-	-	3	7.69	2.13	24.14
4	-	-	-	4	-	-	-
6	13.63	4.74	33.33	5	-	-	-
7	4.54	0.80	21.79	7	61.53	42.53	77.57
SRC = 7	ND = 43						
DST	%	LB	UB				
1	4.65	1.28	15.45	-	-	-	-
2	20.93	11.42	35.20	-	-	-	-
3	11.62	5.07	24.47	-	-	-	-
4	6.97	2.40	18.60	-	-	-	-
5	-	-	-	-	-	-	-
6	-	-	-	-	-	-	-

Table A.2: Similar to Table A.1, but for the L_{30} drifter dataset (see section 2.4).

SRC = 1	ND = 64			SRC = 2	ND = 57		
DST	%	LB	UB	DST	%	LB	UB
2	78.12	66.56	86.49	1	5.26	1.80	14.36
3	51.56	39.58	63.36	3	71.92	59.16	81.92
4	18.75	11.06	29.97	4	38.59	27.06	51.57
5	-	-	-	5	-	-	-
6	-	-	-	6	1.75	0.31	9.29
7	3.12	0.86	10.69	7	3.50	0.96	11.92
SRC = 3	ND = 56			SRC = 4	ND = 50		
DST	%	LB	UB	DST	%	LB	UB
1	1.78	0.31	9.44	1	-	-	-
2	5.35	1.83	14.60	2	-	-	-
4	51.78	39.01	64.33	3	-	-	-
5	1.78	0.31	9.44	5	4	1.10	13.46
6	1.78	0.31	9.44	6	2	0.35	10.49
7	1.78	0.31	9.44	7	2	0.35	10.49
SRC = 5	ND = 22			SRC = 6	ND = 26		
DST	%	LB	UB	DST	%	LB	UB
1	-	-	-	1	7.69	2.13	24.14
2	4.54	0.80	21.79	2	11.53	4.00	28.97
3	-	-	-	3	15.38	6.14	33.53
4	-	-	-	4	15.38	6.14	33.53
6	27.27	13.15	48.15	5	-	-	-
7	13.63	4.74	33.33	7	61.53	42.53	77.57
SRC = 7	ND = 43						
DST	%	LB	UB				
1	11.62	5.07	24.47	-	-	-	-
2	23.25	13.15	37.74	-	-	-	-
3	18.60	9.74	32.61	-	-	-	-
4	11.62	5.07	24.47	-	-	-	-
5	-	-	-	-	-	-	-
6	-	-	-	-	-	-	-

Table A.3: Similar to Tables A.1 and A.2 but for the L_{45} drifter dataset (see section 2.4).

SRC = 1						SRC = 2					
DST	%	LB	UB	TAVG	TSTD	DST	%	LB	UB	TAVG	TSTD
2	90.72	90.34	91.09	6.54	5.16	1	-	-	-	-	-
3	85.27	84.80	85.72	12.97	5.75	3	97.30	97.09	97.50	6.50	3.61
4	13.27	12.84	13.72	23.29	4.11	4	24.71	24.16	25.27	20.12	5.02
5	0.49	0.41	0.59	24.77	1.33	5	1.16	1.03	1.31	25.61	3.41
6	-	-	-	-	0	6	0.15	0.10	0.21	22.37	2.98
7	0.39	0.32	0.48	18.62	5.10	7	-	-	-	-	-
SRC = 3						SRC = 6					
DST	%	LB	UB	TAVG	TSTD	DST	%	LB	UB	TAVG	TSTD
1	-	-	-	-	-	1	0.05	0.03	0.09	27.54	2.81
2	0.02	0.01	0.05	28.5	0.64	2	3.54	3.31	3.79	25.48	2.71
4	65.93	65.32	66.54	11.44	5.22	3	20.96	20.44	21.49	21.95	5.00
5	3.90	3.65	4.15	21.66	4.35	4	13.64	13.20	14.08	24.50	3.62
6	0.09	0.05	0.13	19.06	5.72	5	-	-	-	-	-
7	0.10	0.07	0.15	18.76	1.98	7	12.94	12.52	13.38	12.21	4.91
SRC = 7											
DST	%	LB	UB	TAVG	TSTD						
1	28.28	27.70	28.86	18.35	7.15						
2	47.21	46.57	47.86	17.86	5.48						
3	40.16	39.53	40.80	21.22	4.35						
4	0.74	0.63	0.85	25.17	3.37						
5	-	-	-	-	-						
6	-	-	-	-	-						

Table A.4: Connection percentages and transit times computed from the virtual particle L_{30} dataset. In each panel the source (SRC) and destination (DST) are indicated along with the connection percentage (%), equivalent to the number of particles that left one region and entered another. The 95% confidence intervals were computed using the Wilson score and are indicated in the columns labeled LB and UB. The average and standard deviation of particle transit times are shown in columns labeled TAVG and TSTD, respectively.

SRC = 1						SRC = 2					
DST	%	LB	UB	TAVG	TSTD	DST	%	LB	UB	TAVG	TSTD
2	95.36	95.08	95.63	8.04	8.37	1	-	-	-	-	-
3	90.75	90.37	91.12	14.45	8.12	3	97.60	97.39	97.79	6.59	3.92
4	21.79	21.26	22.33	28.00	7.10	4	30.04	29.45	30.63	22.74	7.47
5	0.80	0.69	0.92	28.39	4.84	5	2.18	2.00	2.37	29.04	4.85
6	0.02	0.01	0.05	33.56	6.03	6	0.25	0.19	0.32	28.72	8.66
7	0.45	0.37	0.55	20.62	6.91	7	0.04	0.02	0.07	36.08	5.88
SRC = 3						SRC = 6					
DST	%	LB	UB	TAVG	TSTD	DST	%	LB	UB	TAVG	TSTD
1	-	-	-	-	-	1	1.28	1.14	1.43	39.02	4.67
2	0.19	0.14	0.25	36.24	5.25	2	8.42	8.07	8.78	31.34	6.11
4	67.36	66.75	67.96	12.01	6.49	3	37.25	36.62	37.87	28.38	8.62
5	4.36	4.10	4.63	23.32	6.59	4	28.87	28.29	29.46	31.12	7.38
6	0.49	0.41	0.59	33.48	7.84	5	-	-	-	-	-
7	0.19	0.14	0.25	24.94	7.54	7	13.33	12.90	13.78	12.91	6.34
SRC = 7											
DST	%	LB	UB	TAVG	TSTD						
1	41.80	41.17	42.44	24.05	10.38						
2	65.49	64.88	66.10	23.16	9.93						
3	60.83	60.19	61.45	26.58	8.65						
4	5.22	4.94	5.52	36.32	5.99						
5	-	-	-	-	-						
6	-	-	-	-	-						

Table A.5: Similar to Table A.4 but for the virtual particle L_{45} dataset.

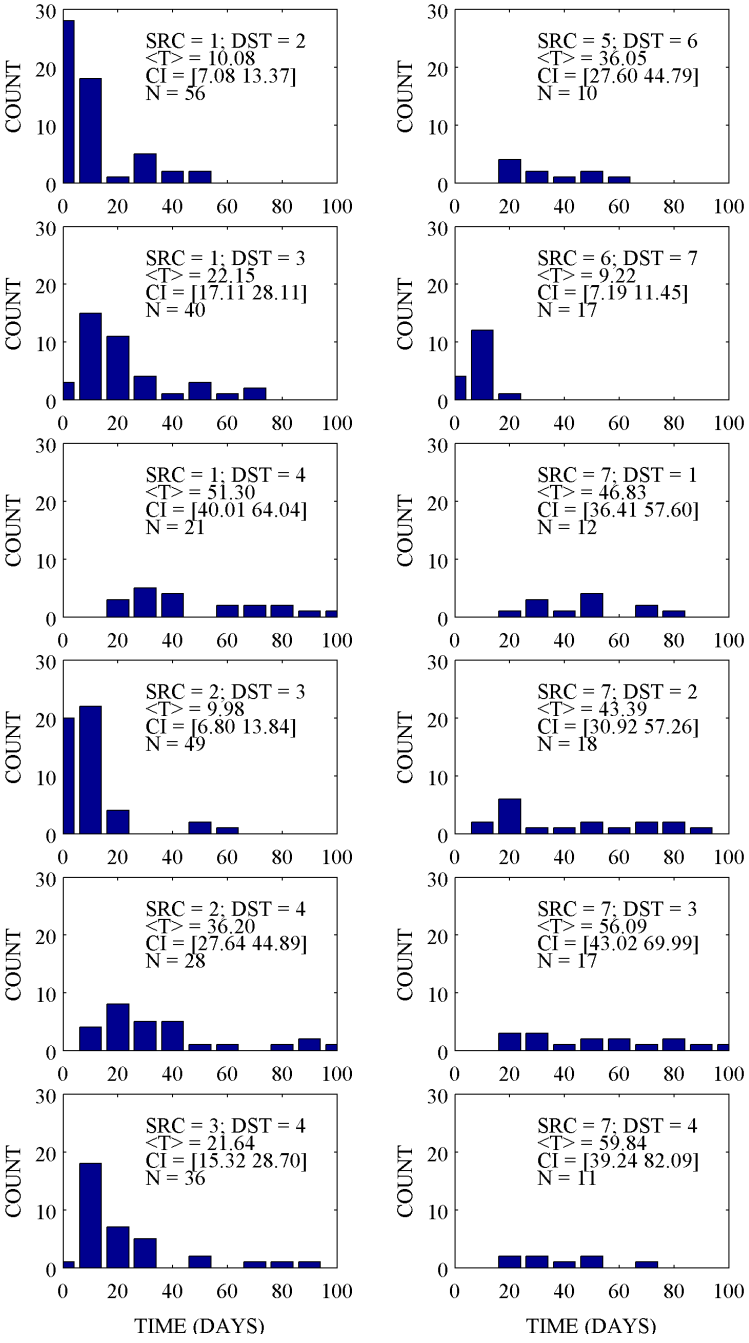

Figure A.13: The histograms of transit times between region pairs connected by at least 10 drifters, with no limitations placed on drifter lifetimes. The source (SRC) and destination (DST) are denoted at the top of each panel, with the bootstrap estimate of the mean ($< T >$) and its corresponding 95% confidence interval (CI = [...]).

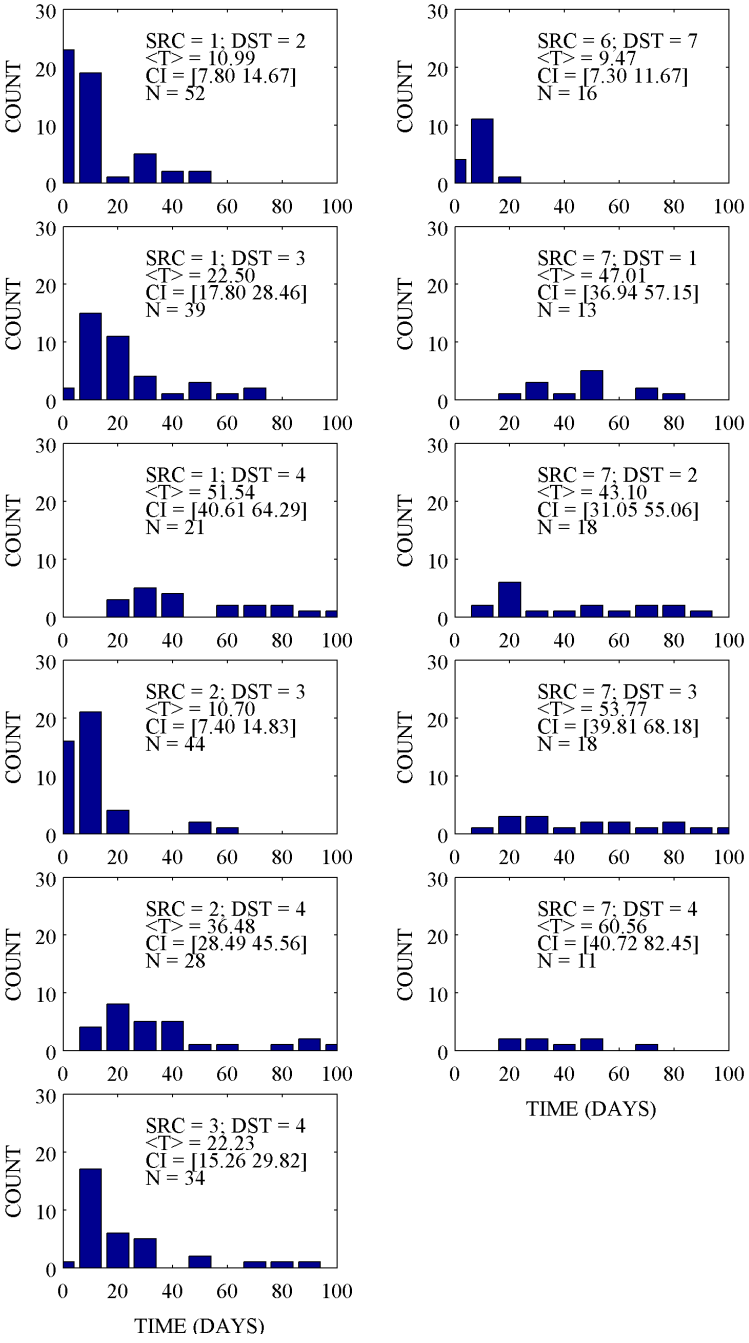

Figure A.14: Similar to Figure A.13 but for histograms of transit times between region pairs connected by at least 10 drifters with lifetimes *at least* 10 days.

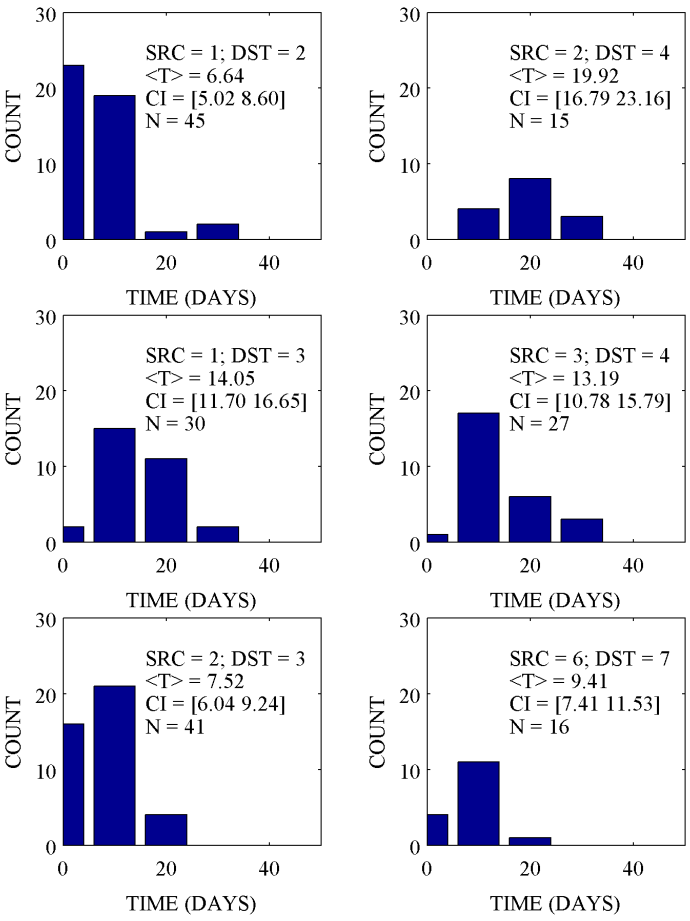

Figure A.15: Similar to Figures A.13 - A.14 but for histograms of transit times between region pairs connected by 10 or more drifters with lifetimes of 10–30 days.

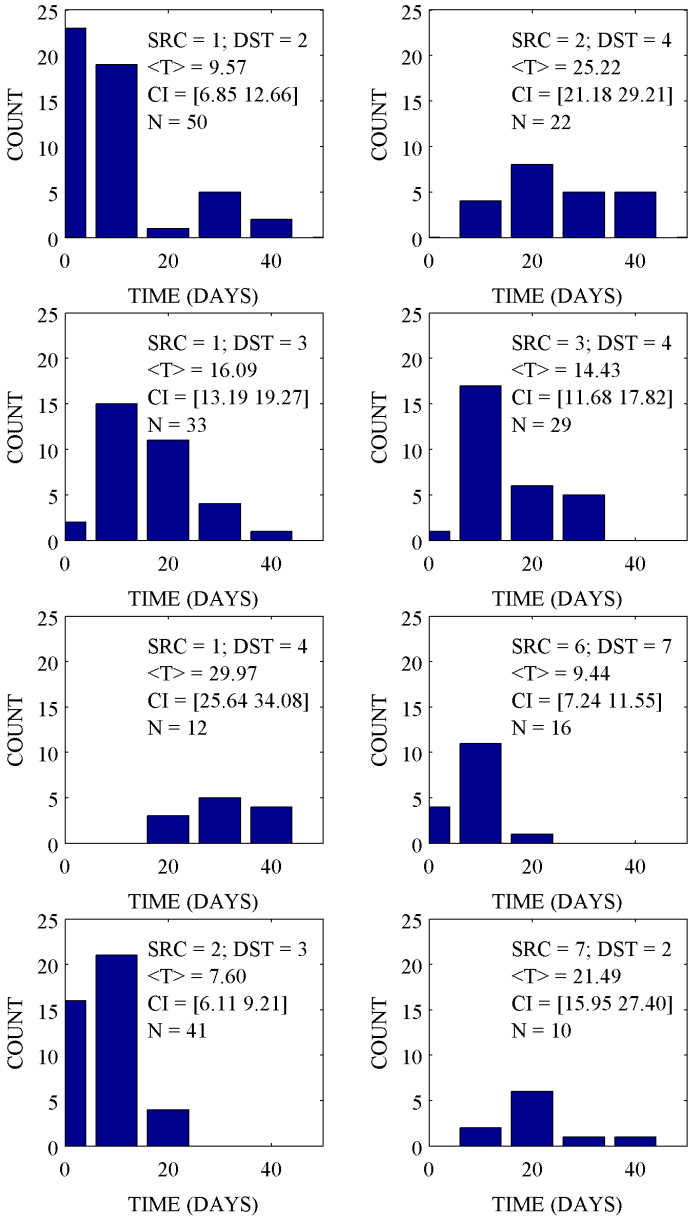

Figure A.16: Similar to Figures A.13 - A.15 but for histograms of transit times between region pairs connected by 10 or more drifters with lifetimes of 10–45 days.

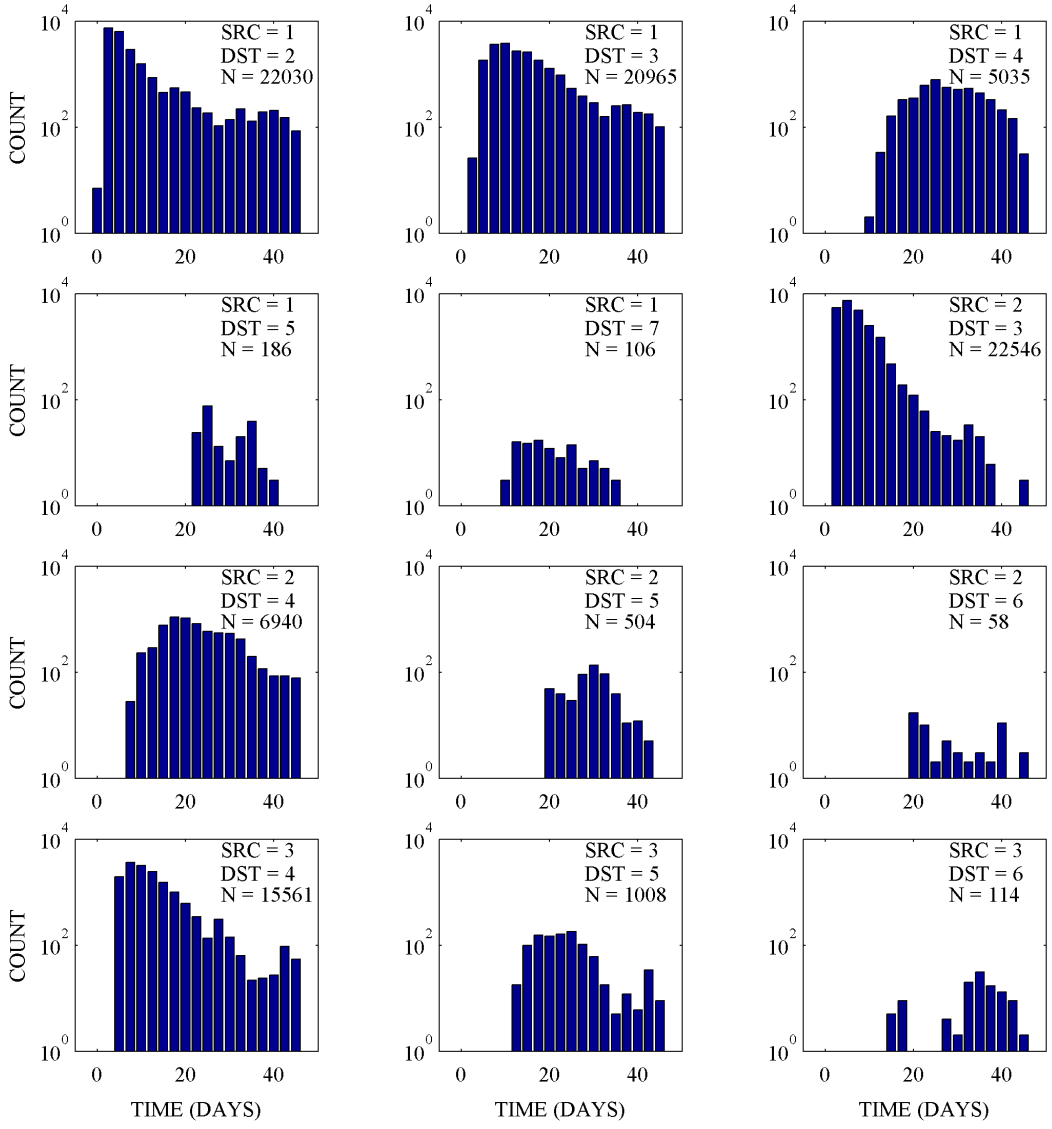

Figure A.17: Part 1 of histograms of transit times between source (SRC) and destination (DST) regions computed from virtual particle trajectories with lifetimes of 45 days with the total number of transit times (N). Note the logarithmic y-axis.

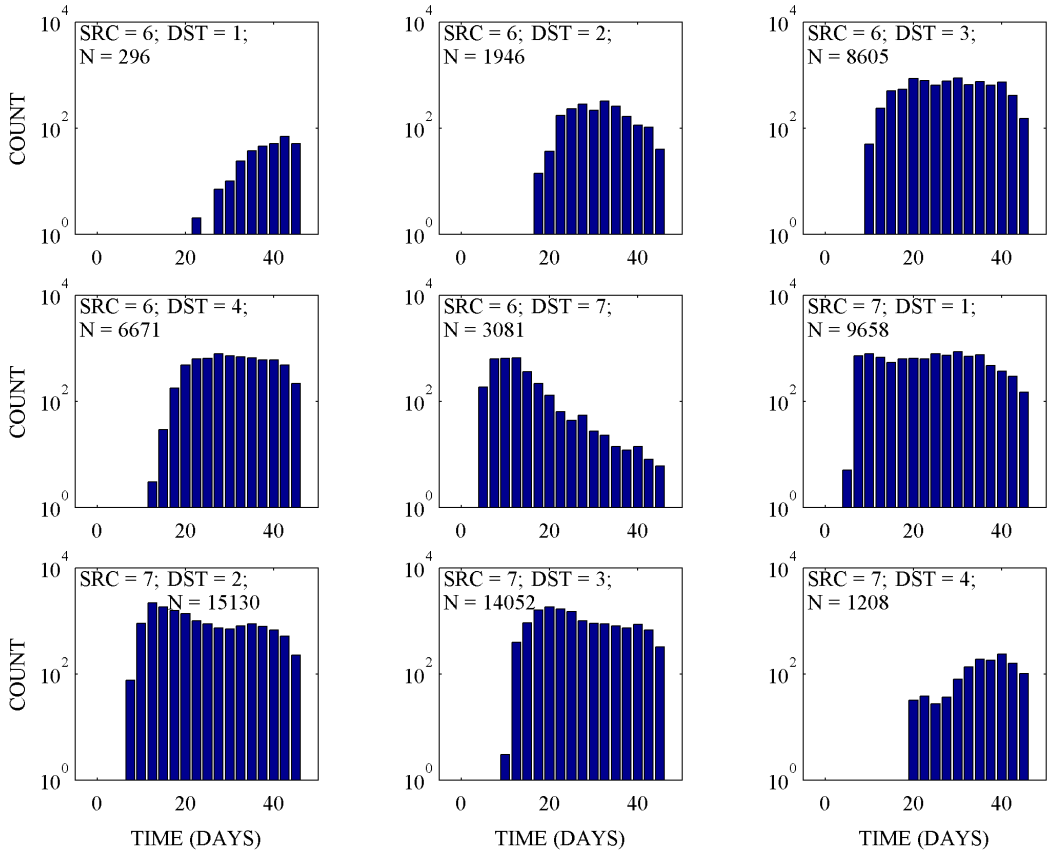

Figure A.18: Continued from Figure A.17, part 2 of histograms of transit times between source (SRC) and destination (DST) regions computed from virtual particle trajectories with lifetimes of 45 days with the total number of transit times (N). Note the logarithmic y-axis.